Lower limb bone structure of Middle Pleistocene hominins from the Caune de l'Arago (Tautavel, France): Evolutionary and functional comparison with the penecontemporaneous hominins of Sima de los Huesos (Atapuerca, Spain)

Tony Chevalier, Marie-Antoinette de Lumley

L'anthropologie xxx (2022) xxx

Available online at www.sciencedirect.com
ScienceDirect
et également disponible sur www.em-consulte.com

Original article

Lower limb bone structure of Middle Pleistocene hominins from the Caune de l'Arago (Tautavel, France): Evolutionary and functional comparison with the penecontemporaneous hominins of Sima de los Huesos (Atapuerca, Spain)

La structure des os du membre inférieur des Hommes du Pléistocène moyen de la Caune de l'Arago (Tautavel, France) : perspectives évolutionnaires et fonctionnelles dans le contexte des hominines pénécontemporains de la Sima de los Huesos (Atapuerca, Espagne)

Tony Chevalier [a,*,b], Marie-Antoinette de Lumley [b,c]

[a] *Université de Perpignan via Domitia, 52, avenue Paul-Alduy, 66100 Perpignan, France*
[b] *UMR 7194 CNRS, Histoire Naturelle de l'Homme Préhistorique (HNHP, MNHN), Centre européen de recherches préhistoriques, avenue Léon-Jean-Grégory, 66720 Tautavel, France*
[c] *Institut de paléontologie humaine, fondation Albert-Ier, Prince-de-Monaco, 1, rue René-Panhard, 75013 Paris, France*

ARTICLE INFO

Article history:
Received 22 July 2022
Accepted 22 July 2022
Available online xxx

Keywords:
Homo
Mobility
Bone cross-section

ABSTRACT

The Caune de l'Arago (Arago) and Sima de los Huesos (Sima) human bones from the European Middle Pleistocene are penecontemporaneous, although the Sima hominins are closely related to Neandertal, and Arago hominins present more archaic features. In previous and in press studies, the cross-sectional geometric properties (CSG) of lower limb bones of Arago and Sima have been studied separately without comparative analyses. Here, in order to bridge this gap, we use the same criteria for both samples to highlight evolutionary affinities and

* Corresponding author at: Université de Perpignan via Domitia, 52, avenue Paul-Alduy, 66100 Perpignan, France.
E-mail addresses: tony.chevalier@cerptautavel.com (T. Chevalier), malumley@mnhn.fr (M.-A. de Lumley).

https://doi.org/10.1016/j.anthro.2022.103065

Femur
Tibia
Fibula

to compare their level and pattern of mobility. This study focuses on the femur, fibula and tibia from Arago and Sima with references to fossils from the sites of Trinil, Zhoukoudian and Lazaret, and ancient and recent *Homo sapiens* (including athletes and non-athletes). We analyze the cross-sectional areas, biomechanical bone "shape" indices (Ix/Iy, Imax/Imin) and pattern of cortical bone distribution. All lower limb bones from Arago have noticeably high to very high relative cortical areas and low to very low medullary areas. The overall femoral pattern in Arago, like Sima, is similar to that of Middle Pleistocene hominins (e.g., low femoral shape indices, Ix/Iy) and Neandertals (e.g., large cross-sectional size). However, the femoral midshaft in Sima presents prominent posteromedial cortical thickening, as a result of a spiral cortical reinforcement along the medial side of the diaphysis. This characteristic is specific to Neandertal and some Middle Pleistocene hominins. In contrast, the midshaft femoral pattern in Arago is close to that of some *Homo erectus*. We also note that the femoral cross-sectional size and relative cortical area in Arago differ drastically to the small size and low relative cortical area of Lazaret and Trinil hominins. The very high shape index at midshaft (i.e., high Imax/Imin) of the Arago tibia is observed in ancient *H. sapiens* and runners; the tibial posterior "pilaster" is found in Neandertals and ancient *H. sapiens*; and the flat or convex tibial faces are similar to Neandertals. Furthermore, the Arago fibulas show marked fibular posterolateral cortical reinforcement with low anteroposterior strengthening. These leg features (tibia, fibula) are also found in some Sima hominins (but not in all individuals). Consequently, this study confirms the presence of archaic features in Arago and the close evolutionary relationship between Sima and Neandertal. This proposition is mainly based on the femoral midshaft pattern influenced by the pelvofemoral complex, considered to be substantially genetically controlled. The leg functional analysis highlights a high level of mobility and travelling in uneven terrains or in mountainous areas in Arago, consistent with known environments and hunting practices. Previously, an analogous hypothesis was proposed put forward for Sima hominins.

RÉSUMÉ

Mots clés :
Homo
Mobilité
Fémur
Tibia
Fibula
Section transversale de l'os

Les os humains de la Caune de l'Arago (Arago) et de la Sima de los Huesos (Sima) appartenant au Pléistocène moyen européen sont considérés comme pénécontemporains. Toutefois, les Hommes de la Sima ont de fortes affinités avec les Néandertaliens, et ceux de l'Arago présentent des traits plus archaïques. Dans les études précédentes et celles en cours de parution, les propriétés géométriques des sections transversales des os du membre inférieur de l'Arago et de la Sima ont été étudiées séparément sans analyse comparative entre elles. Ici, nous allons combler ce manque en utilisant les mêmes critères pour les deux échantillons afin de mettre en évidence les affinités évolutives de ces deux groupes ainsi que leur niveau et leur type de mobilité. Cette étude se focalise sur le fémur, la fibula et le tibia de l'Arago et ceux de la Sima, avec un échantillon supplémentaire concernant principalement les Hommes de Trinil, Zhoukoudian et du Lazaret, ainsi que les *Homo sapiens* anciens et récents (incluant des athlètes). Nous analysons les aires des sections transversales, l'indice de « forme » biomécanique (Ix/Iy, Imax/Imin) et le modèle de distribution de l'os cortical. De manière remarquable, nous notons que tous les os

Please cite this article in press as: Chevalier, T., de Lumley, M.-A., Lower limb bone structure of Middle Pleistocene hominins from the Caune de l'Arago (Tautavel, France): Evolutionary and

du membre inférieur de l'Arago possèdent une aire corticale relative élevée à très élevée, et une aire médullaire petite à très petite. Le modèle fémoral général à l'Arago est similaire à celui de la Sima, et partage des traits anatomiques avec les Hommes du Pléistocène moyen (ex., faibles indices fémoraux, Ix/Iy) et les Néandertaliens (ex., grandes sections transversales). Toutefois, la portion fémorale mi-diaphysaire à la Sima présente un épaississement cortical proéminent dans la zone postéro-médiale, résultant du renforcement cortical en spiral se déployant le long de la région interne de la diaphyse. Une telle caractéristique est typique des Néandertaliens et de certains fémurs du Pléistocène moyen. En revanche, le modèle fémoral de l'Arago à mi-diaphyse est similaire à celui observé sur certains *Homo erectus*. Nous notons également que l'aire totale des sections fémorales et l'aire corticale relative à l'Arago diffèrent drastiquement de celles des fémurs du Lazaret et de Trinil, pour lesquelles les valeurs sont très faibles. De la jambe, nous notons que le tibia de l'Arago présente un indice de forme très élevé (c.-à-d., très haut Imax/Imin), identique à ceux des *H. sapiens* anciens et des coureurs à pied; un « pilastre » tibial postérieur, fréquemment identifié chez les Néandertaliens et les *H. sapiens* anciens; et des faces du tibia plates à convexes, comme chez les Néandertaliens. Enfin, la fibula de l'Arago se caractérise par un fort renforcement cortical postérolatéral et un faible étirement antéropostérieur. Ces caractéristiques de la jambe (tibia, fibula) ont aussi été identifiées sur certains os des Hommes de la Sima (mais pas sur tous les individus). En conséquence, cette étude confirme la présence de traits archaïques sur le squelette des Hommes de l'Arago, et la proximité évolutive entre les Hommes de la Sima et les Néandertaliens. Cette proposition est principalement fondée sur le modèle structural fémoral mi-diaphysaire dont les caractéristiques prennent forme sous l'impact du complexe pelvo-fémoral, soumis à une forte influence génétique. L'analyse fonctionnelle de la jambe a mis en évidence un haut niveau de mobilité chez les Hommes de l'Arago, ainsi que des déplacements sur des terrains irréguliers ou montagneux, en cohérence avec l'environnement de cette grotte et la pratique de la chasse. Précédemment, une hypothèse analogue a été émise pour les Hommes de la Sima.

1. Introduction

The Caune de l'Arago[1] (Tautavel, France) and Sima de los Huesos[2] (Atapuerca, Spain) hominins are two key samples in the European Middle Pleistocene evolutionary context. They are penecontemporaneous and chronologically precede Neandertals and *Homo sapiens* (Arnold et al., 2014; Clark et al., 2003; Couchoud, 2006; Falguères et al., 2015; Grün et al., 2008; Rink et al., 1995; Valladas et al., 2008; see also Richter et al., 2017; Roksandic et al., 2022). The two human groups share cranial and postcranial characteristics with Middle Pleistocene hominins, and contrast with ancient

[1] Arago.
[2] Sima.

Please cite this article in press as: Chevalier, T., de Lumley, M.-A., Lower limb bone structure of Middle Pleistocene hominins from the Caune de l'Arago (Tautavel, France): Evolutionary and

H. sapiens. Morphologically, the hominins from Sima are more closely related to Neandertal than to the more archaic Arago remains (Arsuaga et al., 2014, 2015; Bermúdez de Castro et al., 2018; Chevalier and Lumley, 2018, 2022a; Lumley, 2015, 2022; Martinón-Torres et al., 2012; Rodríguez et al., 2018; Rosas et al., 2002). Chevalier and Lumley (2022a, b, c)[3], Chevalier (2022) and Rodríguez et al. (2018) recently included the Arago and Sima samples in the well-known evolutionary pattern of lower limb structural properties (i.e., cross-sectional geometric properties, CSG) (e.g., Trinkaus and Ruff, 2012) providing taxonomic and behavioral information. However, no CSG comparative analysis of Arago and Sima hominins has been carried out to date. In addition, the femoral CSG of Sima were not compared to those of Trinil (Ruff et al., 2015a) and Lazaret (Chevalier and Lumley, 2018), two major sites in the evolutionary context of the Asian and European Middle Pleistocene.

To summarize Chevalier and Lumley (2022a, b, c), Chevalier (2022) and Rodríguez et al. (2018), Arago and Sima hominins show many similar lower limb bone features to Early and Middle Pleistocene hominins, and to some extent to Neandertals: ovoid femoral subtrochanteric cross-section; high cortical thickness and low medullary cavity; low femoral ratio of the second moment of area (I_x/I_y; diaphyseal "shape" index) and absence of pilaster (which strongly contrasts with the ancient *H. sapiens* pattern); femoral medial cortical reinforcement at midshaft (see also Chevalier et al., 2015; Puymerail et al., 2012a, b; Ruff et al., 2015a; Trinkaus and Ruff, 2012). Authors also note in Arago and Sima hominins, close femoral robusticity to that of Neandertal, well-defined and marked fermoral subtrochanteric fossa, convex or flat cross-sectional contours of tibial diaphysis (contrasting with ancient *H. sapiens*, as mentioned in Trinkaus and Ruff, 2012) and thick cortical bones and high second polar moment of area in the midshaft fibular cross-sections (Arsuaga et al., 2015; Chevalier and Lumley, 2022a, b, c; Rodríguez et al., 2018). Finally, physical behaviour can be specifically inferred from the tibia and fibula morphology of hominin samples from Sima and Arago. Chevalier (2022) and Rodríguez et al. (2018) suggest a high level of mobility and travelling probably on uneven terrain.

The main results of previous studies are insufficient for a rigorous analysis of the similarities and differences between the bone properties of lower limb bones of Arago and Sima hominins. Furthermore, some descriptions are specific to studies of Arago and Sima hominins. For example, femoral midshaft cortical thickness distribution was not analysed in Rodríguez et al. (2018), although posteromedial reinforcement is a frequent structural pattern in Neandertal and some Middle Pleistocene hominins (Chevalier et al., 2015), and consequently an expected characteristic in the Sima femoral sample, as shown for one Sima individual in Chevalier and Lumley (2018, 2022a). The fibula is a very rare bone in ancient periods and it is conducive to functional investigation (Hart et al., 2020; Lüscher et al., 2019; Marchi, 2007, 2015; Marchi et al., 2019; Marchi and Shaw, 2011; Sparacello et al., 2014, 2018), but the comparative analysis of the Sima fibulas is not very thorough, and some comparisons based on structural parameters are also lacking in the fibular study of Arago, such as the midshaft relative cortical area and pattern of cortical distribution.

The main objective of this new study is to compare the bone structural pattern of the lower limb (femur, tibia, fibula) of Arago and Sima hominins and determine whether one of these groups is closer to Neandertal than the other one and whether different pattern and level of mobility co-exist during the European Middle Pleistocene. Here, we focus on the comparison of cross-sectional geometric properties between four partial femurs, one partial tibia and five partial fibulas from Arago (Chevalier and Lumley, 2022a, b, c) (Figs. 1–3) with the Sima sample (Rodríguez et al., 2018). The comparative analysis includes the cross-sectional areas, relative cortical area, relative bending rigidity (biomechanical shape indices) and pattern of cortical distribution. Biomechanical robusticity is not included as it requires the estimation of bone length and body mass, two variables difficult to estimate for the Arago human remains (but see discussion below and propositions in Chevalier, 2022). Note that the comparative analyses are from updated measurements of Arago postcranial bones taken from x-ray micro computed tomography (Micro-CT) scanning, and not from medical CT scan imaging as in previous studies (Chevalier and Lumley, 2018, 2022a, b, c). Furthermore, we present unedited cross-sectional properties of one fibula (A152) recently found in Arago Cave. We will also examine the femurs from Lazaret (Chevalier and Lumley, 2018) and Trinil (Ruff et al., 2015a), as the CSGs of these

[3] The monograph of the human remains from the Caune de l'Arago is currently in press with the publisher. It is scheduled for release in 2022.

Please cite this article in press as: Chevalier, T., de Lumley, M.-A., Lower limb bone structure of Middle Pleistocene hominins from the Caune de l'Arago (Tautavel, France): Evolutionary and

Fig. 1. Femurs from the Caune de l'Arago. All bones are in posterior view except the natural cross-sections from the proximal part of A141 for which the posterior side is upward. Note the very small medullary area in A141.
Fémurs de la Caune de l'Arago. Tous les os sont présentés en vue postérieure, excepté les sections transversales naturelles provenant de la portion proximale, pour lesquelles la face postérieure est dirigée vers le haut. Notez la très petite cavité médullaire de A141.

bones have not yet been, or only poorly compared, with the human remains of Arago and Sima (Chevalier and Lumley, 2022a; Rodríguez et al., 2018).

2. Material and method

2.1. Material

This study focuses mainly on the Middle Pleistocene hominins from the Caune de l'Arago (Arago, Table 1, Figs. 1–3) and Sima de los Huesos (Sima) sites, and secondarily on Neandertals and ancient *H. sapiens* samples, and femurs from Trinil, Lazaret and Zhoukoudian (Table 2). Recent *H. sapiens* samples are used for functional inference and to complete data analysed in previous studies. They include fibulas and tibias of athletes and non-athletes.

The Arago sample includes femurs (A48, A53, A57, A141), tibias (A120) and fibulas (A49, A52/A56, A125, A144, A152) (Table 1, Figs. 1–3). These bones come from the major unit G, correlate with marine

Fig. 2. Tibia from the Caune de l'Arago. The tibia A120 is presented in medial (left) and anterior (right) views.
Tibia de la Caune de l'Arago. Le tibia A120 est présenté avec les vues médiale (à gauche) et antérieure (à droite).

isotopic stage 12, and date to about 438 ± 31ka based on ESR and U-series dating (Falguères et al., 2015). The selection of these bones from the Arago corpus was based on the comparability of cross-sectional properties with those of Sima de los Huesos (Rodríguez et al., 2018). For example, the immature fibulas (A33) and the supposedly adult fibulas (A104, A114) were not used. The femurs A48 and A57 could belong to the same individual given their morphology and size. Potentially, we have six fibulas (A33, A49, A52-A56, A104-A152, A114-A125, A144), with a minimum of four individuals (Chevalier and Lumley, 2022c). Some propositions are in contradiction with their location in the archaeological level, but the sublevels in the unit G are compressed on top of each other. Unit G is an impressive accumulation of bones and lithic artefacts attaining a depth of one metre (Lumley, 2015). The sublevels represent potential levels, but it is not possible to clearly delimit them over the whole area. It is thus possible that a bone attributed to one level actually come from a contiguous level.

For the Middle Pleistocene sample from Sima, we used the bones presented in Rodríguez et al. (2018): femur (F-IX, X, XI, XIII, XIV, XVI, AT-1020); tibia (TIB-I, III, IV, VI, XI, XII, AT-848); fibula (Fib-I, II, III, AT-1060).

Please cite this article in press as: Chevalier, T., de Lumley, M.-A., Lower limb bone structure of Middle Pleistocene hominins from the Caune de l'Arago (Tautavel, France): Evolutionary and

Fig. 3. Fibulas from the Caune de l'Arago. All fibulas are in lateral/posterolateral views, except A144 in anterior view.
Fibulas de la Caune de l'Arago. Toutes les fibulas sont présentées en vue latérale/postérolatérale, excepté A144, présentée en vue postérieure.

Table 1
Hominins lower limb bones from Arago (Caune de l'Arago). Only the postcranial remains included in this study are presented in this table. In Arago Cave, three other femurs (A17, A38, A51), one other tibia (A95-A96), and three other fibulas (A33, A104, A114) have also been found. The major unit G is divided into sublevels (Gs1, Gm1, Gm2, Gi4), the most recent is Gs1.
Os du membre inférieur des Hommes de la Caune de l'Arago. Seuls les restes postcrâniens inclus dans cette étude sont présentés dans ce tableau. Dans la grotte de l'Arago ont été trouvés trois autres fémurs (A17, A38, A51), un autre tibia (A95-A96), et trois autres fibulas (A33, A104, A114). La grande unité G est composée de sous-unités (Gs1, Gm1, Gm2, Gi4), la plus récente étant Gs1.

Type of bone	Specimen	Laterality	Major unit	Archaeostratigraphical unit
Femur	A48	Right	G	Gs1
	A53	Right	G	Gi4
	A57	Left	G	Gm2
	A141	Right	G	Gm2
Tibia	A120	Left	G	Gs1
Fibula	A49	Right	G	Gs1
	A52-A56	Right	G	Gm3
	A125	Left	G	Gs1
	A144	Left	G	Gm2
	A152	Left	G	Gm2

Please cite this article in press as: Chevalier, T., de Lumley, M.-A., Lower limb bone structure of Middle Pleistocene hominins from the Caune de l'Arago (Tautavel, France): Evolutionary and

Table 2
Fossil samples used for the comparative analysis of cross-sectional properties: femur, tibia and fibula.
Echantillon fossile utilisé pour l'analyse comparative des propriétés géométriques des sections transversales : fémur, tibia et fibula.

Samples				
Femur	80%	65%	50%	35%
Caune de l'Arago	A48, A57, A141	A48, A57, A141	A141	A53, A141
Sima de los Huesos	F-X, F-XI, F-XIII, F-XIV, F-XVI, AT-1020	F-X, F-XI, F-XIII, F-XIV, AT-1020	F-IX, F-X, F-XIII, F-XIV, F-XVI	F-IX, F-X, F-XIII
Lazaret	Laz 13, Laz 17	Laz 13, Laz 17	Laz 17, Laz 25	Laz 15, Laz 25
Trinil	Femur II, Femur III, Femur IV	Femur II, Femur III, Femur IV	Femur II, Femur IV	Femur II, Femur III, Femur IV, Femur V
Neandertals	Amud 1, La Chaise, Chapelle-aux-Saints, Feldhofer 1, La Ferrassie 1, 2, Krapina 213, 214, Saint Césaire (Roche-à-Pierrot), Spy 2, Tabun 1	Amud 1, La Chaise-de-Vouthon/Tour1, Feldhofer 1, La Ferrassie 1, 2, Fond-de-Forêt, Krapina 257.32, 257.33, Palomas 52, 92, 96, La Quina 38, Shanidar 6, Spy 2	Amud 1, La Chaise BD5, Chapelle-aux-Saints, Feldhofer 1, Ferrassie 1, 2, Fond-de-Forêt 1, Palomas 96, Quina 5, Rochers-de-Villeneuve 1, Saint-Césaire 1, Shanidar 4, 5, 6, Spy 2, Tabun 1, 3, CDV-Tour1, Les Pradelles	Amud 1, Chapelle-aux-Saints, Feldhofer 1, Ferrassie 1, 2, Fond-de-Forêt 1, Spy 2, Tabun 1
Ancient *Homo sapiens*	Qafzeh 8, 9, Skhul 4, 5, 6, 9, La Rochette 2, Cro-magnon 1 (4323, 4325), 4322, Arene Candide 1, Barma Grande 2, Grotte des enfants 4, Paglicci 25, Veneri 1,2, Mladeč 27, 28, Paviland 1, Pavlov 1, Dolní Věstonice 3, 13, 14, 16, 35, Sunghir 1, 4, Nahal 'En-Gev 1, Ohalo 2, Minatogawa 1, 2, 3, 4, Tianyuan 1	Qafzeh 6, 8, 9, Skhul 4, 5, Cro-magnon 1, 4322, 4324, Mladeč 27, 28, Paviland 1, Pavlov 1, Dolní Věstonice 3, 13, 14, 16, 41, Sunghir 1, 4, Nahal 'En-Gev 1, Ohalo 2, Minatogawa 1, 3, 4, Tianyuan 1, Willendorf 1	Qafzeh 3, 8, 9, Skhul 3, 4, 5, 6, 7, Arene Candide 1, Barma Grande 2, Cro-magnon 1, 4322, 4324, Dolní Věstonice 3, 13, 14, 16, 35, Grotte des Enfants 4, Minatogawa 1, 2, 3, 4, Mladeč 27, Nahal 'En-Gev 1, Ohalo 2, Paglicci 25, Paviland 1, Pavlov 1, Rochette 2, Sunghir 1, 4, Veneri 1, 2, Willendorf 1, Zhoukoudian-UC 67, 68	Qafzeh 9, Skhul 4, 5, 6, 7, Cro-magnon 1, 4322, 4328, Dolní Věstonice 3, 13, 14, 16, 40, Minatogawa 1, 3, 4, Mladeč 27, Nahal 'En-Gev 1, Ohalo 2, Paviland 1, Pavlov 1, Sunghir 1, 4

TIBIA	65%	50%	35%
Caune de l'Arago	A120	A120	A120
Sima de los Huesos	TIB-I, TIB-III, TIB-VI, TIB-XII, AT-848	TIB-I, TIB-III, TIB-IV, TIB-VI, TIB-XI, TIB-XII, AT-848	TIB-I, TIB-III, TIB-IV, TIB-VI, TIB-XI, TIB-XII, AT-848
Neandertals	Amud 1, Chapelle-aux-Saints, Ferrassie 1, 2, Shanidar 2, Spy 2	Amud 1, Chapelle-aux-Saints, Ferrassie 1, 2, Krapina 257.15, 257.20, Oliveira 4, Palomas 96, Saint Césaire 1, Shanidar 2, 6, Spy 2, Tabun 1	Amud 1, Chapelle-aux-Saints, Ferrassie 1, 2, Palomas 96, Shanidar 2, Spy 2, Tabun 1
Ancient *Homo sapiens*	Qafzeh 3, Skhul 4, 5, 6, Cro-magnon 4330, 4332, Dolní Věstonice 3, 13, 14, 15, 16, Minatogawa 3, 4, Minatogawa 4, Ohalo 2, Paviland 1, Sunghir 1	Qafzeh 8, 9, Skhul 4, 5, 6, Arene Candide 1, Cro-magnon 4330, 4332, 4333, Dolní Věstonice 3, 13, 14, 15, 16, Grotte des Enfants 4, Minatogawa 1, 3, 4, Ohalo 2, Paviland 1, Sunghir 1, Tianyuan 1, Veneri 1, 2	Qafzeh 8, Skhul 3, 4, 5, 6, Cro-magnon 4330, 4331, 4332,Dolní Věstonice 3, 13, 14, 15, 16, Minatogawa 3, 4, Nahal 'En-Gev 1, Ohalo 2, Paviland 1, Sunghir 1, Tianyuan 1

FIBULA	50%
Caune de l'Arago	A49, A52-A56, A125, A144, A152
Sima de los Huesos	Fib-I, Fib-II, Fib-III, AT-1060
Neandertals	La Ferrassie 1
Ancient *Homo sapiens*	Caviglione, Cro-Magnon 4334, 4335, Abri Pataud 58-2-37817 R

The Trinil (Femur II, III, IV, V), Lazaret (Laz 13, 15–17, 25) and Zhoukoudian (1, 2, 4, 5, 6) samples are only composed of femurs. Neandertals and ancient *H. sapiens* samples are represented mainly by femurs and tibias, with one Neandertal (La Ferrassie 1) and four Upper Paleolithic (Caviglione, Cro-Magnon 4334, 4335, Abri Pataud 58-2-37817 R) fibulas.

Considerable additional data for *H. sapiens* femurs and tibias are from Ruff (2018a) and shared by Christopher Ruff in the European dataset (previously at https://fae.johnshopkins.edu/chris-ruff/). We also used recent *H. sapiens* samples from Shaw and Stock (2009a), Marchi and Shaw (2011), including tibial and fibular CSGs from athletes (cross-country runners, field hockey players) and a control group (non-athletes). Finally, our sample comprises the recent *H. sapiens* fibular sample (individuals of known age) presented in Chevalier and Tignères (2020).

3. Methods

It is essential to observe the internal structure for our study. To achieve our objectives, (1) we scanned bones from Arago and Caviglione, and recent *H. sapiens* for this study and other projects; (2) we used microtomographic data from Sébastien Villotte and the Muséum National d'Histoire Naturelle de Paris (MNHN), and data and illustrations found in the literature (see references in the text). The quantitative and qualitative analyses are from cross-sections for which we measured the CSGs and described cortical bone distribution.

Here, we present information about the scanners used to take our own measurements.

The Arago bones stored at the EPCC (Tautavel, France) were scanned at the ISIS4D X-ray platform (In Situ Innovative Set-ups) of the university of Lille (France), using an RX-Solution UltraTom micro-CT scanner. Isotropic voxel sizes reconstructions were 72–50 μm for the femurs, 62 μm for the tibia and 43–19 μm for the fibulas.

The fibulas of Caviglione and recent *H. sapiens* stored at Musée de l'Homme (Paris) were scanned at the AST-RX platform of the MNHN (Paris, France), using a GE Sensing & Inspection Technologies phoenix|X-ray v|tome|x L240-180 micro-CT scanner. Isotropic voxel sizes reconstructions were 105 μm for Caviglione and 136 μm for recent *H. sapiens* (Georges Olivier's collection). This latter was previously analysed in Chevalier and Tignères (2020).

The micro-CT scan of the Neandertal fibula from La Ferrassie 1 were made available by MNHN (Paris, France). This bone was scanned at the AST-RX platform. Isotropic voxel sizes reconstructions were 100 μm.

Micro-CT scans of Cro-Magnon and Abri Pataud fibulas were made available by Sébastien Villotte (Thibeault and Villotte, 2018; Villotte et al., 2017). These bones were scanned at the AST-RX platform. Isotropic voxel sizes reconstructions were 89–126 μm.

The cross-sections are selected as a percentage of bone length (80%, proximal; 65%, mid-proximal; 50%, midshaft; 35%, mid-distal). Biomechanical length was chosen for femur and tibia (e.g., Trinkaus and Ruff, 2012), while maximal length was used for the fibula (Chevalier and Tignères, 2020). However, this method is not directly applicable when bones are not whole, as at Arago. We selected the cross-section level based on anatomical features (e.g., entheses, foramen, diaphyseal shape) and recommendations in Trinkaus and Ruff (2012), and by direct comparison with whole bone (see details in Chevalier and Lumley, 2022a, b, c). Note that a relatively well-preserved femur (A141) and fibula (A144) were very useful to making appropriate choices for other Arago bones. The femoral biomechanical length of A141 is about 416 mm and the fibular maximal length of A144 is about 370 mm (Figs. 1, 3) (Chevalier, 2022; Chevalier and Lumley, 2022a, c).

We used Avizo 7.1.0 (FEI Visualization Sciences Group, Hillsboro) to extract the cross-sections and ImageJ 1.51q software (National Institutes of Health; http://rsbweb.nih.gov/ij/) (Schneider et al., 2012) associated with the plugin MomentMacro (http://www.hopkinsmedicine.org/fae/mmacro.html/, provided for free download by Dr. Christopher Ruff) to quantify the structural parameters of the Arago bones, the femur from Lazaret at 65%, and fibulas of ancient and recent *H. sapiens* (except the athletes and control data presented in Marchi and Shaw, 2011; Shaw and Stock, 2009a).

The structural parameters (i.e., CSG) are the total area (TA, mm^2), medullary area (MA, mm^2), cortical area (CA, mm^2), relative cortical area (%CA), second moments of area about ML (Ix, mm^4) and AP (Iy, mm^4) axis, minimal (Imin, mm^4) and maximal (Imax, mm^4) second moments of area, polar

moment of area (J, mm^4). These parameters represent mechanical performances (See Ruff, 2018b; Ruff and Hayes, 1983a). The cortical area, second moment of area and polar second moment of area reflect compressive/tensile strength, bending rigidity and torsional and average bending rigidity, respectively. We added the theta angle for two well-preserved femurs from Arago and Sima. It represents the direction of the greatest bending rigidity, measured from the mediolateral axis. The positive angles were taken clockwise. The angle (theta) of F-X (Sima) was measured from the cross-sections presented in Rodríguez et al. (2018).

CSGs of Early and Middle Pleistocene hominins (except Arago, and data at 65% in Lazaret), Neandertals and ancient *H. sapiens* are from Chevalier et al. (2015), Chevalier and Lumley (2018), Puymerail et al. (2012a, b), Rodríguez et al. (2018), Ruff et al. (2015a) and Trinkaus and Ruff (2012). CSGs of athletes and the control group are from Shaw and Stock (2009a) and Marchi and Shaw (2011).

In the two latter studies, the fibular cross-section is located at 50% of tibial biomechanical length and is slightly more proximal than the 50% of fibular maximal length. To evaluate the consequences on our analysis, we proposed measurements for recent fibulas at 50% and 60% of fibular maximal length. Finally, we selected individuals in our recent fibular sample for some analyses given the age-dependence of some structural parameters, as shown in Chevalier and Tignères (2020).

The comparative analysis of midshaft cortical distribution in the lower limb bone of Arago and Sima is based on our own micro-CT scan imaging for Arago and the cross-sections illustrated in Rodríguez et al. (2018) for Sima. To highlight the cortical distribution pattern along the femoral diaphysis in Arago (A141) and Sima (F-X), we added mapping of bone cortical thickness with the Bob Dougherty's "Local Thickness" plugin included in the BoneJ Plugin implemented in ImageJ, "which defines the thickness at a point as the diameter of the greatest sphere that fits within the structure and which contains the point" (Dougherty and Kunzelmann, 2007; Hildebrand and Rüegsegger, 1997).

Statistical analyses were performed using PAST version 2.14 and 4.08 (Hammer et al., 2001). Given the small sample size of Arago hominins, we do not propose comparative statistical tests.

4. Results

CSG data of Arago bones are given in Tables 3–5.

4.1. Femoral CSG

In general, the femurs from Arago (A48, A53, A57, A141) present high total area and relative cortical area and low medullary area and Ix/Iy, compared to hominin fossils. The total area and relative bending rigidity (Ix/Iy and Imax/Imin) in Sima are close to Arago (Table 6, Fig. 4).

The femoral total area of Arago and Sima (Table 6, Fig. 4) are close at 65% and 50% (midshaft) of biomechanical bone length. However, proximal and distal locations show distinct results. They may depend on the ability to select 80% and 35% locations on fragmentary bones and the high variation of size in these regions. The femoral total areas of Arago and Sima are higher than Neandertal, but relatively close to the latter, and contrast sharply with the small cross-sections of Lazaret, Trinil and Zhoukoudian. The ancient *H. sapiens* bones present intermediate values between these two groups.

The medullary area of Arago femurs (Table 6, Fig. 4) is particularly small at 65% and 50%. The cross-section at 50% of Arago and Zhoukoudian differs drastically from that of the other groups (including Sima), which present higher values. The smallest medullary area in Sima at 50% is twice as large as that of Arago (A141). The medullary area at 35% is very distinct for Arago and Sima, with very high values for the latter.

The relative cortical area (Table 6, Fig. 4) is very high in Arago from 65% to 35%. Only Zhoukoudian hominins show close values to Arago at midshaft. Femurs from Sima present lower values than Arago (except at 80%). The highest value at midshaft in Sima is 82.4% (See in Rodríguez et al., 2018). The only known midshaft relative cortical area in Arago is 92% (A141). The more distal the cross-section, the greater the difference between Arago and Sima. From 80% to 50%, Sima is similar to Neandertal. In contrast, Trinil and Lazaret show a very low relative cortical area.

Please cite this article in press as: Chevalier, T., de Lumley, M.-A., Lower limb bone structure of Middle Pleistocene hominins from the Caune de l'Arago (Tautavel, France): Evolutionary and

Table 3
Femoral cross-sectional geometric properties: Arago. Individual data, mean and standard deviation (in brackets). TA: total area (mm^2); CA: cortical area (mm^2); TA-CA: medullary area (mm^2); %CA: relative cortical area; Ix: second moment of area about mediolateral axis (mm^4); Iy: second moment of area about anteroposterior axis (mm^4); Imax: maximum second moment of area (mm^4); Imin: minimum second moment of area (mm^4); J: polar second moment of area (mm^4); Zp: polar section modulus (mm^3).
Propriétés géométriques des sections transversales du fémur : Arago. Données individuelles, moyennes et écarts-types (entre parenthèses). TA : aire totale (mm^2) ; CA : aire corticale (mm^2) ; TA-CA : aire médullaire (mm^2) ; %CA : aire corticale relative ; Ix : second moment d'aire selon l'axe médio-latéral (mm^4) ; Iy : second moment d'aire selon l'axe antéro-postérieur (mm^4) ; Imax : second moment d'aire maximal (mm^4) ; Imin : second moment d'aire minimal (mm^4) ; J : second moment d'aire polaire (mm^4) ; Zp : module de section polaire (mm^3).

Location/ specimen	TA	CA	TA-CA	%CA	Ix	Iy	Ix/Iy	Imax	Imin	Imax/Imin	J	Zp
80%												
A48	792	587	205	74.1	37,136	57,940	0.64	58,269	36,807	1.58	95,076	5286
A57	798	611	187	76.6	37,320	61,444	0.61	62,459	36,305	1.72	98,764	5301
A141	838	666	172	79.5	47,600	63,198	0.75	69,955	40,844	1.71	110,798	5708
Mean	809 (25)	621 (41)	188 (10)	76.7 (2.7)	40,685 (5988)	60,860 (2677)	0.67 (0.07)	63,561 (5920)	37,985 (2488)	1.67 (0.08)	101,546 (8222)	5432 (239)
65%												
A48	649	592	58	91.1	29,635	37,463	0.79	37,475	29,622	1.27	67,098	4227
A57	667	607	60	91.1	30,587	40,358	0.76	40,403	30,542	1.32	70,945	4381
A141	685	637	48	93.0	32,213	44,926	0.72	49,041	28,098	1.75	77,139	4484
Mean	667 (18)	612 (23)	55 (6.0)	91.7 (1.1)	30,812 (1304)	40,916 (3763)	0.76 (0.04)	42,306 (6013)	29,421 (1234)	1.45 (0.26)	71,727 (5066)	4364 (129)
50%												
A141	645	594	52	92.0	28,491	38,596	0.74	38,684	28,403	1.36	67,087	4144
35%												
A53	740	515	225	69.6	40,031	39,697	1.01	45,303	34,425	1.32	79,728	4682
A141	672	553	119	82.3	31,395	39,058	0.80	40,566	29,887	1.36	70,453	4345
Mean	706 (48)	534 (27)	172 (75)	76.0 (9.0)	35,713 (6107)	39,378 (452)	0.91 (0.15)	42,935 (3350)	32,156 (3209)	1.34 (0.03)	75,091 (6558)	4514 (238)

Table 4
Tibial cross-sectional geometric properties: Arago. Individual data, mean and standard deviation (in brackets). Meaning of abbreviations and units in legend Table 3.
Propriétés géométriques des sections transversales du tibia : Arago. Données individuelles, moyennes et écarts-types (entre parenthèses). Voir la signification des abréviations et les unités dans la légende du Tableau 3.

Location	TA	CA	TA-CA	%CA	Ix	Iy	Ix/Iy	Imax	Imin	Imax/Imin	J	Zp
A120-65%	577.9	466.1	111.8	80.7	42,156	16,262	2.60	43,390	15,027	2.90	58,418	3166
A120-50%	535.3	462.0	73.0	86.3	36,074	14,740	2.45	37,157	13,657	2.72	50,814	2921
A120-35%	480.0	380.0	100.0	79.2	24,110	13,696	1.76	25,249	12,557	2.01	37,806	2441

Table 5
Fibular cross-sectional geometric properties at midshaft: Arago. Individual data, mean and standard deviation (in brackets). Meaning of abbreviations and units in legend Table 3.
Propriétés géométriques des sections transversales de la fibula : Arago. Données individuelles, moyenne et écart-type (entre parenthèses). Voir la signification des abréviations et les unités dans la légende du Tableau 3.

	TA	CA	TA-CA	%CA	Ix	Iy	Ix/Iy	Imax	Imin	Imax/Imin	J	Zp
A49	160	137	23.0	85.6	2178	2564	0.85	3152	1590	1.98	4742	485
A52-56	166	137	29.7	82.2	1889	2649	0.71	2961	1577	1.88	4538	497
A125	161	135	26.4	83.6	2209	2123	1.04	2702	1630	1.66	4332	479
A144	161	131	30.1	81.3	1694	2676	0.63	2744	1626	1.69	4370	431
A152	141	124	16.8	88.1	1658	1730	0.96	1987	1402	1.42	3389	388
Mean	158	133	25.2	84.2	1926	2348	0.84	2709	1565	1.73	4274	456
	(10)	(5)	(5.5)	(2.7)	(260)	(412)	(0.17)	(442)	(94)	(0.22)	(521)	(46)

Considering the exceptional relative cortical area at midshaft in Arago (A141), we added supplementary data mainly from *H. sapiens* (Fig. 5). A large sample comes from the *H. sapiens* data of Ruff and colleagues (Ruff, 2018a) with 1830 individuals from the Upper Palaeolithic to the twentieth century. We completed this sample with 61 individuals belonging to the *Homo* genus ranging from the Early Pleistocene to the Upper Pleistocene (Chevalier et al., 2015; Chevalier and Lumley, 2018; Puymerail et al., 2012a, b; Rodríguez et al., 2018; Ruff et al., 2015a; Trinkaus and Ruff, 2012). Only two individuals have a higher relative cortical area than that of femur A141. Although the Fig. 5 shows a trend of decreasing relative cortical area from the oldest to the most recent human groups, if we break down our *non-sapiens* sample, we observe very low values in some localities (Trinil and Lazaret). The relative cortical areas of Lazaret and Trinil are close to the more recent *H. sapiens*, which have the lowest relative cortical area. Consequently, collectively, the femurs from Lazaret, Trinil, Sima, Neandertal, Zhoukoudian and Arago present the same range of variation as *H. sapiens*. Note also that only 12 individuals from the *H. sapiens* sample (N = 1830) present a lower medullary area than A141, although 1622 individuals have a total area lower than A141.

The femurs from Arago present low relative bending rigidity (Ix/Iy) with similar overall pattern to Sima along the diaphysis, although the Arago values are lower (Table 6, Fig. 4). The best discrimination between all samples is observed at 50% where Arago is similar to Zhoukoudian. Trinil, Neandertal and Lazaret show higher indices at 50%, but all groups are clearly distinct from ancient *H. sapiens*. This latter has very elevated indices between 65% and 35%, with the maximal value at 50%. From the Imax/Imin index at 50%, A141 belongs to the middle group with Trinil, Neandertal, Sima and Zhoukoudian, and differs from the lower values found in Lazaret and the higher values in ancient *H. sapiens*. Such clear differences do not exist at 65% and 35%.

4.2. Tibial CSG

In general, the tibia from Arago (A120) presents a high relative cortical area and Imax/Imin index, and low medullary area along the diaphysis compared to hominin fossils. Arago is not particularly

Table 6
Femoral cross-sectional geometric properties: all samples. Mean and standard deviation (in brackets). Meaning of abbreviations and units in legend Table 3. References: Chevalier et al. (2015), Chevalier and Lumley (2018), Rodríguez et al. (2018), Ruff et al. (2015a), Trinkaus and Ruff (2012). Arago and Lazaret (65%) data are from this study.
Propriétés géométriques des sections transversales du fémur : tous les échantillons. Moyennes et écarts-types (entre parenthèses). Voir la signification des abréviations et les unités dans la légende du Tableau 3. Références : Chevalier et al. (2015), Chevalier et Lumley (2018), Rodríguez et al. (2018), Ruff et al. (2015a), Trinkaus et Ruff (2012). Les données de l'Arago et du Lazaret (65 %) sont de cette étude.

	N	TA	TA-CA	%CA	Ix/Iy	Imax/Imin
80%						
Arago	3	809 (25)	188 (17)	76.7 (2.7)	0.67 (0.07)	1.67 (0.08)
Sima de los Huesos	6	716 (139)	160 (58)	78.2 (4.4)	0.71 (0.16)	1.68 (0.19)
Lazaret	2	583 (81)	185 (28)	67.6 (9.3)	0.61 (0.08)	1.73 (0.14)
Trinil	3	579 (14)	177 (22)	69.5 (3.1)	0.59 (0.09)	1.73 (0.28)
Neandertal	11	734 (150)	181 (95)	76.3 (8.8)	0.78 (0.14)	1.51 (0.30)
Ancient Homo sapiens	33	649 (136)	159 (60)	75.9 (6.9)	0.74 (0.17)	1.87 (0.37)
65%						
Arago	3	667 (18)	55 (6.0)	91.7 (1.1)	0.76 (0.04)	1.45 (0.26)
Sima de los Huesos	5	651 (145)	86 (38)	87.2 (3.2)	0.83 (0.17)	1.42 (0.23)
Lazaret	2	523 (119)	109 (21)	79.1 (0.8)	0.82 (0.04)	1.34 (0.08)
Trinil	3	549 (24)	135 (42)	75.6 (6.4)	0.82 (0.11)	1.42 (0.19)
Neandertal	14	612 (119)	91 (5.5)	85.4 (5.5)	0.84 (0.2)	1.45 (0.30)
Ancient Homo sapiens	26	592 (121.8)	104 (46.0)	82.6 (6.1)	1.10 (0.23)	1.37 (0.15)
50%						
Arago	1	645	52	92.0	0.74	1.36
Sima de los Huesos	5	701 (135)	144 (33)	79.5 (2.9)	0.82 (0.11)	1.42 (0.19)
Lazaret	2	514 (141)	130 (16)	74.2 (4.0)	1.01 (0.16)	1.15 (0.00)
Trinil	2	540 (27)	141 (18)	74.0 (2.0)	0.88 (0.22)	1.36 (0.45)
Zhoukoudian	5	502 (46)	63 (19)	87.6 (3.0)	0.76 (0.08)	1.43 (0.06)
Neandertal	19	642 (121)	125 (36)	80.4 (5.2)	0.93 (0.13)	1.31 (0.18)
Ancient Homo sapiens	37	596 (119)	137 (45)	77.1 (6.6)	1.47 (0.36)	1.57 (0.32)
35%						
Arago	2	706 (48)	172 (75)	76.0 (9.0)	0.91 (0.15)	1.34 (0.03)
Sima de los Huesos	3	846 (116)	363 (27)	56.8 (3.1)	1.11 (0.08)	1.21 (0.08)
Lazaret	2	601 (139)	275 (87)	62 (0.0)	0.88 (0.07)	1.18 (0.05)
Trinil	4	537 (31)	185 (14)	65.5 (2.6)	1.09 (0.08)	1.32 (0.28)
Neandertal	8	688 (80)	217 (37)	68.4 (4.1)	1.12 (0.14)	1.28 (0.16)
Ancient Homo sapiens	23	623 (117)	222 (80)	64.8 (10.0)	1.27 (0.27)	1.36 (0.22)

close to Sima, except that both samples present the classical tibial pattern with a decrease in Imax/Imin from 65% to 35% (Table 7, Fig. 6).

More particularly, the tibial total area in Arago (Table 7, Fig. 6) is close to ancient *H. sapiens* and Neandertal (except at 65% for this latter). The tibias from Sima present higher values and are similar to Neandertal at 65%.

The tibial medullary areas in Arago (Table 7, Fig. 6) are very small at 65% and 50%. Note that the value of one individual in Sima (TIB-IV) is smaller than Arago at 50%. Generally, the other groups present similar means to each other.

The tibial relative cortical area in Arago (Table 7, Fig. 6) is very elevated at 65% and 50% and close to other groups at 35%. Arago contrasts with Sima, Neandertal and ancient *H. sapiens*, which present strong similarities at 50% and 35%. However, TIB-IV from Sima presents a value close to Arago at 50% (84.7% *versus* 86.3%).

We propose the same approach for the relative cortical area as for the femur. We added supplementary data mainly from *H. sapiens* (Fig. 7). A large sample comes from the *H. sapiens* data of Ruff and colleagues (Ruff, 2018a) with 1651 individuals from the Upper Palaeolithic to the twentieth century. We completed this sample with 33 individuals belonging to the *Homo* genus ranging from the Early Pleistocene to the Upper Pleistocene (Rodríguez et al., 2018; Trinkaus and Ruff, 2012). Fifty-four individuals show a more elevated relative cortical area than A120 (N = 51/1651; 3/33). Note also that

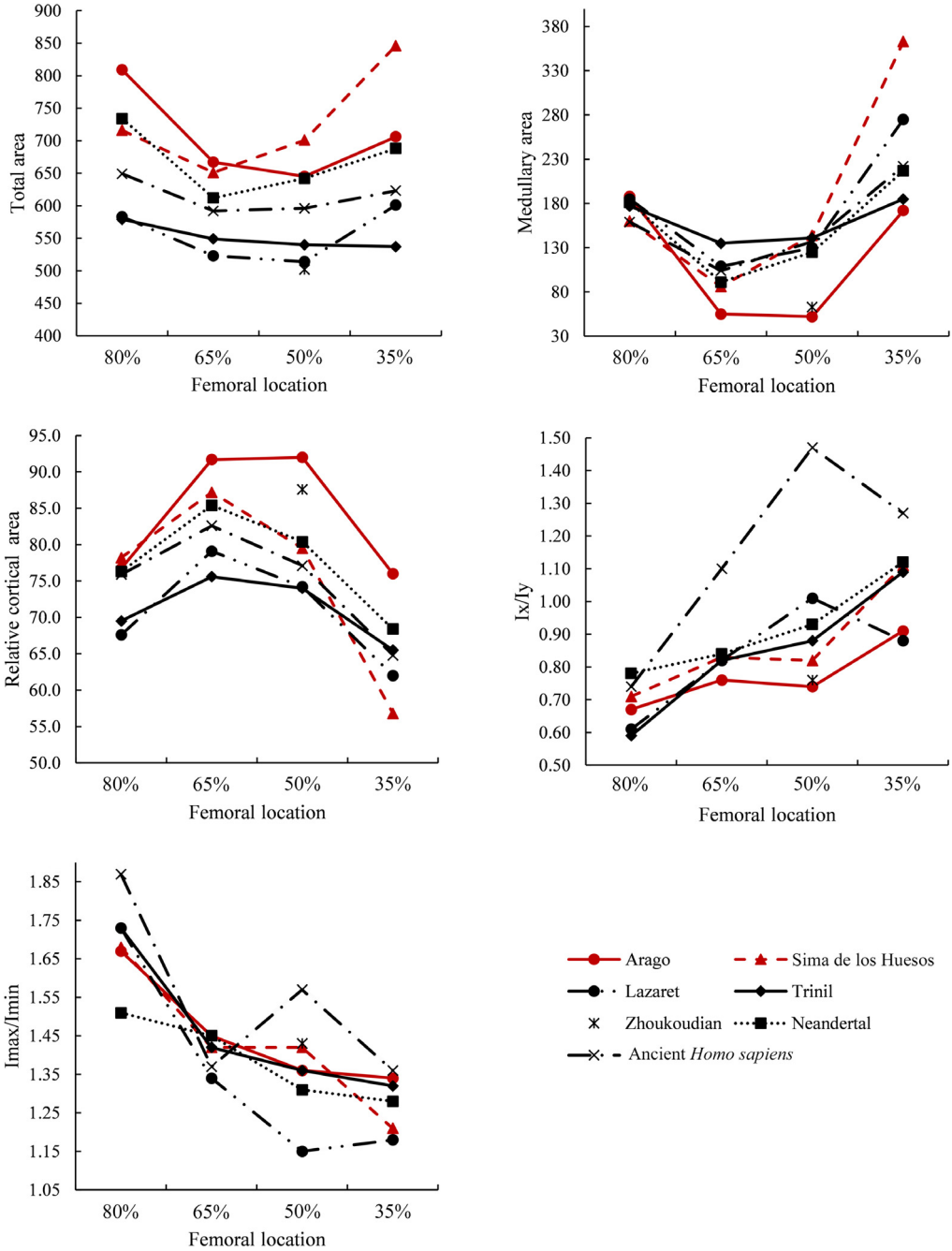

Fig. 4. Femoral cross-sectional geometric properties: hominin fossils (mean values). Arago hominins are represented by three individuals at 80% and 65%, one individual at 50% and two individuals at 35%. See units in legend Table 3.
Propriétés géométriques des sections transversales du fémur : les hominines fossiles (valeurs moyennes). Les Hommes de l'Arago sont représentés par trois individus pour les sections à 80 % et 65 %, un individu pour la section à 50 %, et deux individus pour la section à 35 %. Voir les unités dans la légende du Tableau 3.

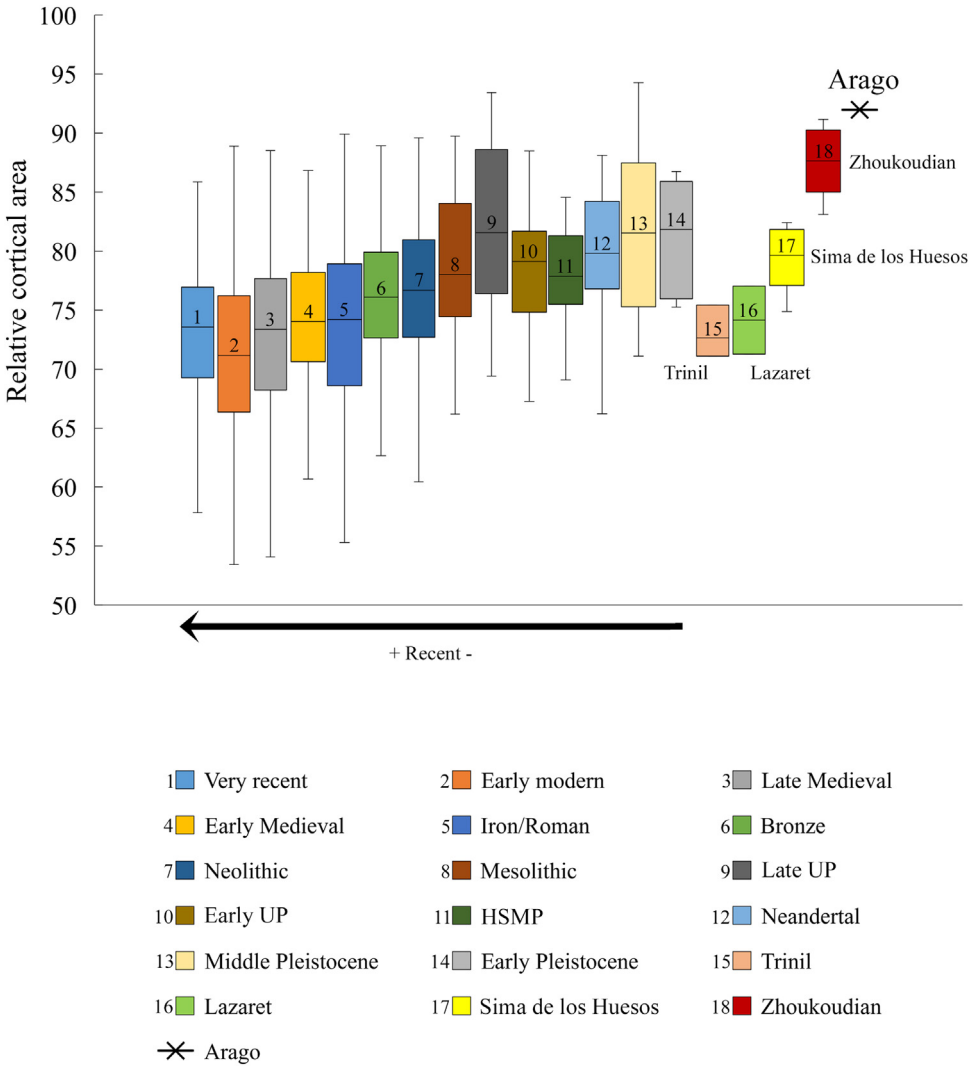

Fig. 5. Femoral relative cortical area (%): Arago *versus Homo* (N = 1891). Middle Pleistocene without Arago hominins. *Homo sapiens* from 1 to 11. UP: Upper Palaeolithic; HSMP: *H. sapiens* Middle Palaeolithic.
Aire corticale relative du fémur (%) : Arago versus Homo *(N = 1891). Les Hommes de la Caune de l'Arago ne sont pas inclus dans le groupe du Pléistocène moyen. Les* Homo sapiens *sont représentés par les groupes numérotés de 1 à 11. UP : Paléolithique supérieur ; HSMP :* H. sapiens *du Paléolithique moyen.*

178 *H. sapiens* individuals (N = 1651) present a lower medullary area than A120, although 1492 individuals have a lower total area than A120.

The relative maximal bending rigidity of the tibia from Arago is higher than Sima and Neandertal, and close to ancient *H. sapiens* (Table 7, Fig. 6).

4.3. Fibular CSG

The hominin fossils (including Arago, Sima, one Neandertal and four ancient *H. sapiens*) present clear differences at midshaft to recent *H. sapiens* (Table 8, Fig. 8). The former group shows higher total

Table 7
Tibial cross-sectional geometric properties: all samples. Mean and standard deviation (in brackets). Meaning of abbreviations and units in legend Table 3. References: Rodríguez et al. (2018), Shaw and Stock (2009a), Trinkaus and Ruff (2012). Arago data are from this study. M: male; F: female.
Propriétés géométriques des sections transversales du tibia : tous les échantillons. Moyenne et écart-type (entre parenthèses). Voir la signification des abréviations et les unités dans la légende du Tableau 3. Références : Rodríguez et al. (2018), Shaw et Stock (2009a), Trinkaus et Ruff (2012). Les données de l'Arago sont de cette étude. M : homme; F : femme.

	N	TA	CA	TA-CA	%CA	J	Imax/Imin
65%							
Arago	1	578		112	80.7		2.89
Sima de los Huesos	5	694 (82)		230 (37)	66.8 (4.2)		2.70 (0.40)
Neandertal	6	673 (68)		228 (74)	65.6 (12)		2.58 (0.36)
Ancient Homo sapiens	16	579 (142)		192 (55)	66.8 (5.8)		2.97 (0.40)
50%							
Arago	1	535	462	73	86.3	50,814	2.72
Sima de los Huesos	7	576 (96)	449 (71)	127 (32)	78.2 (3.7)	56,132 (18,380)	2.18 (0.45)
Neandertal	13	512 (87)	396 (73)	116 (32)	77.3 (5.5)	44,445 (16,337)	2.25 (0.38)
Ancient Homo sapiens	24	524 (123)	409 (100)	116 (40)	77.9 (5.8)	51,939 (21,947)	2.55 (0.60)
Field Hockey-M	17		411 (43)		79.9 (3.3)	46,766 (11,087)	2.22 (0.27)
Runner-M	15		423 (39)		79.5 (2.9)	51,237 (10,586)	2.60 (0.50)
Runner-F	18				77.9 (4.8)		2.53 (0.38)
Control-M	20		364 (43)		74.6 (5.0)	39,462 (7505)	2.28 (0.28)
Control-F	37				72.7 (4.1)		2.02 (0.31)
35%							
Arago	1	480		100	79.2		2.01
Sima de los Huesos	7	516 (90)		110 (11)	78.3 (4.0)		1.61 (0.33)
Neandertal	8	481 (95)		122 (22)	74.0 (4.1)		1.68 (0.29)
Ancient Homo sapiens	20	455 (119)		112 (53)	74.6 (6.7)		2.02 (0.46)

area, relative cortical area, cortical area and polar moment of area and lower medullary area (except Neandertal for this latter variable). The fibulas from Arago (A49, A52/A56, A125, A144, A152) display high total area, polar second moment of area, cortical area and relative cortical area, and low medullary area compared to hominin fossils (including Sima) (Table 8, Fig. 8). Means differences between Arago and Sima are due to frequent higher values and lower standard deviations in Arago. The highest values in Sima are often close to, or even higher than those of Arago, and their medullary areas are close.

4.4. Tibial and fibular CSG: comparisons with athletes

The tibia (A120) from Arago presents high cortical area, relative cortical area and Imax/Imin in comparison to athletes (i.e., runners and field hockey players) and the control group (non-athletes). The polar second moment of area of this bone is close to that of runners and higher than field hockey players, and much higher than the control group. Imax/Imin in Arago is close to female and male runners. It is very different from that of field hockey players and the control group, which present similar values to Sima and Neandertal (Table 7, Fig. 9).

The fibulas from Arago (A49, A52/A56, A125, A144, A152) present high polar second moment of area and cortical area, and very low Ix/Iy compared to athletes and recent non-athletes (control group and other recent *H. sapiens*). The fibulas from Sima also tend to differ from recent *H. sapiens* (athletes and non-athletes), but are closer to them than Arago (Table 8, Fig. 10). Imax/Imin (which do not refer to the mediolateral and anteroposterior axes and do not take into account cross-sectional orientation) show the same trend as in the preceding analysis. However, the differences are less accentuated, and Arago and Sima values are close to those of our recent *H. sapiens* sample. Note that the cross-sectional properties at 60% and 50% of fibular maximal length (Table 8) are close (but not similar) regarding the CSG differences between these two locations in our recent *H. sapiens* sample. Thus, the slightly more proximal location in fibular cross-section for runners, field hockey players and the control group (see methodology in Marchi

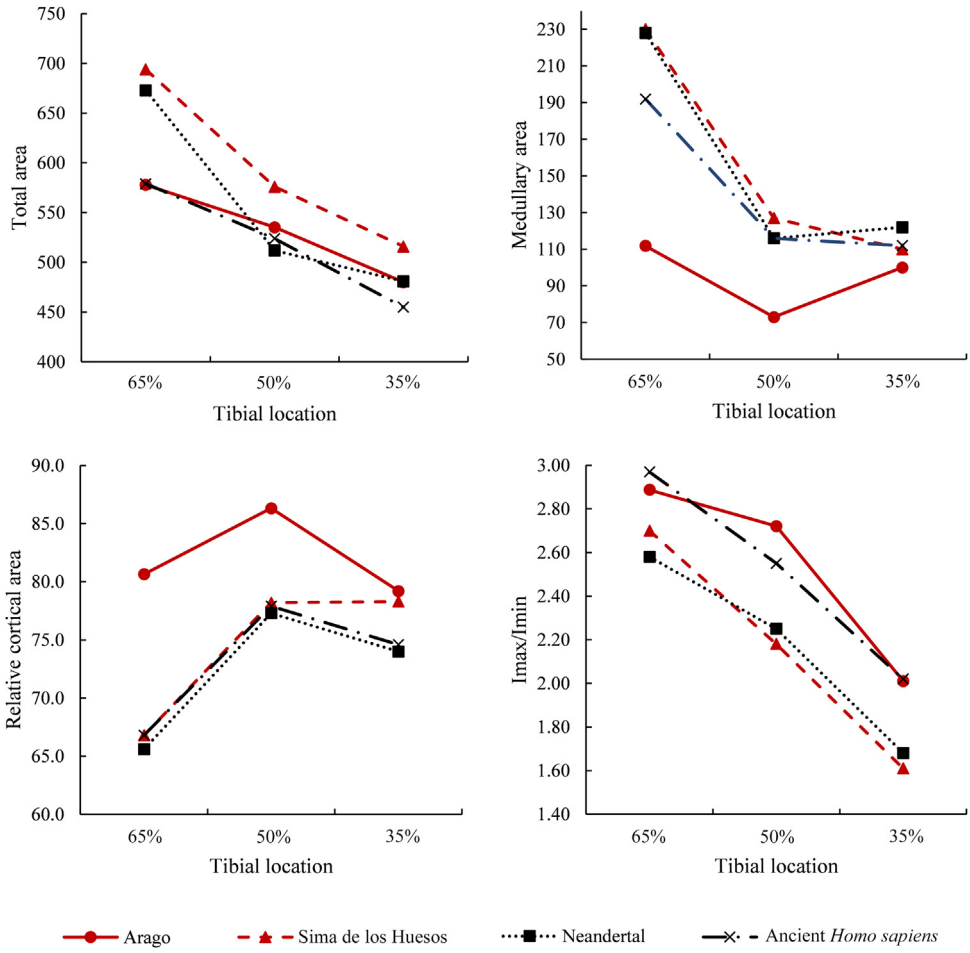

Fig. 6. Tibial cross-sectional geometric properties: hominin fossils (mean values). Arago hominins are represented by one individual. See units in legend Table 3.
Propriétés géométriques des sections transversales du tibia : les hominines fossiles (valeurs moyennes). Les Hommes de l'Arago sont représentés par un seul individu. Voir les unités dans la légende du Tableau 3.

and Shaw, 2011; Shaw and Stock, 2009a), compared to other samples, probably does not impact our comparative analysis interpretation, given the differences observed in our comparative study.

4.5. Pattern of cortical distribution and cross-contour

The femoral cross-section at midshaft in Arago (A141) displays roughly similar cortical bone thickness in each direction. Its cortical bone distribution pattern is close to that of Zhoukoudian (J and 1) and KNMER 1808 (Fig. 11). In contrast, the femurs from Sima show posteromedial cortical reinforcement (i.e., posteromedial bone cortical thickening). This characteristic is associated in some femurs (F-IX and F-X) with thin cortical thickness on the lateral side in comparison to the medial side. Such posteromedial reinforcement is frequent in Neandertals (e.g., Amud I, Fond-de-Forêt, Les Pradelles, La Ferrassie 1) and some European Pleistocene hominins (e.g., Karain, Ehringsdorf) (Chevalier et al., 2015; Chevalier and Lumley, 2018, 2022a) (Fig. 11). Cortical bone distribution in

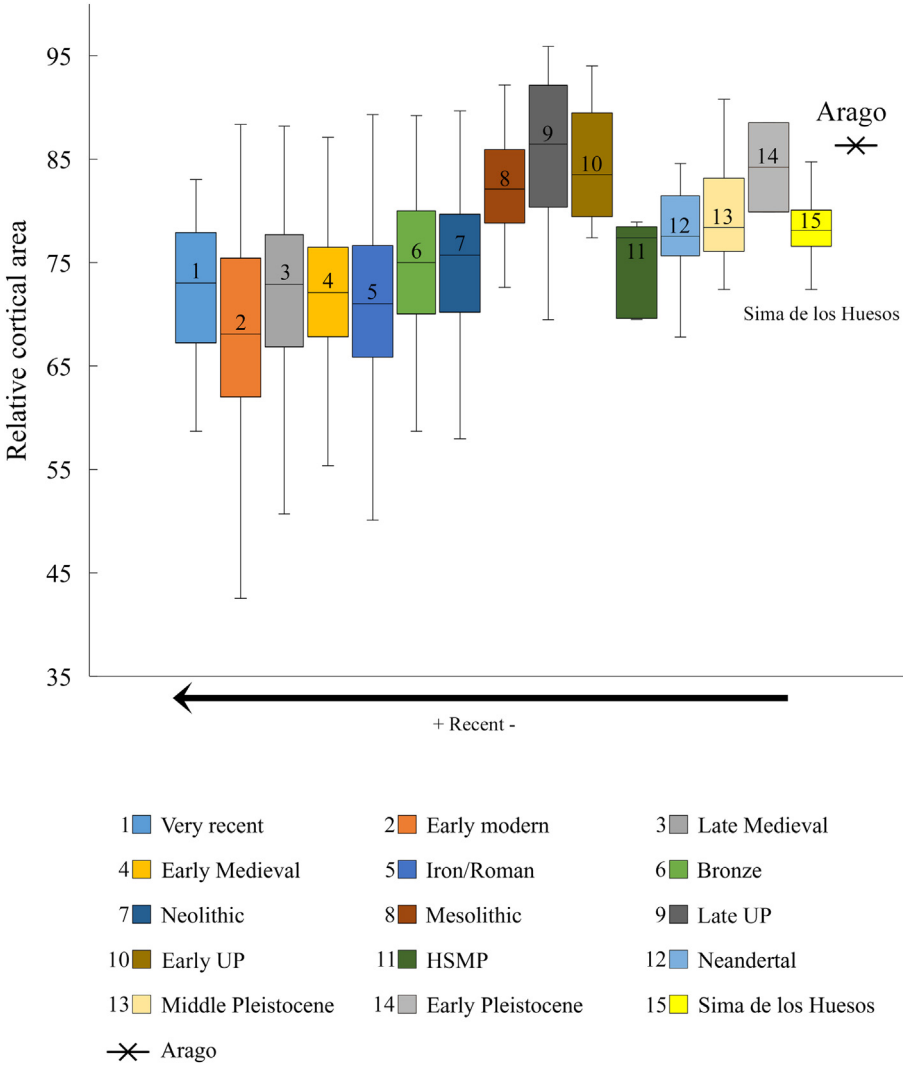

Fig. 7. Tibial relative cortical area (%): Arago *versus Homo* (N = 1684). Middle Pleistocene without Arago hominins. *Homo sapiens* from 1 to 11. UP: Upper Paleolithic; HSMP: *H. sapiens* Middle Paleolithic.
Aire corticale relative du tibia (%) : Arago versus Homo *(N = 1684). Les Hommes de la Caune de l'Arago ne sont pas inclus dans le groupe du Pléistocène moyen. Les* Homo sapiens *sont représentés par les groupes numérotés de 1 à 11. UP : Paléolithique supérieur ; HSMP :* H. sapiens *du Paléolithique moyen.*

Lazaret does not match with Arago or Sima patterns, although the posterior thickening in Lazaret 25 (see in Chevalier and Lumley, 2018) is approximately reminiscent of F-XVI. The pattern of Trinil 4 and 5, with (only) relative thickening on the medial side (without posteromedial thickening) (See in Ruff et al., 2015a), is close to Zhoukoudian and differs to Sima and Neandertals. However, although some patterns and trends were determined, it remains difficult to rigorously classify each *Homo* individual.

Cortical distribution along the femoral diaphysis was observed on two well-preserved femurs from Arago and Sima and four cross-sections at 80%, 65%, 50% and 35% of bone length (Fig. 12). The maximal cortical thickness in Arago (A141) is medial at 80% (with a relatively high lateral value),

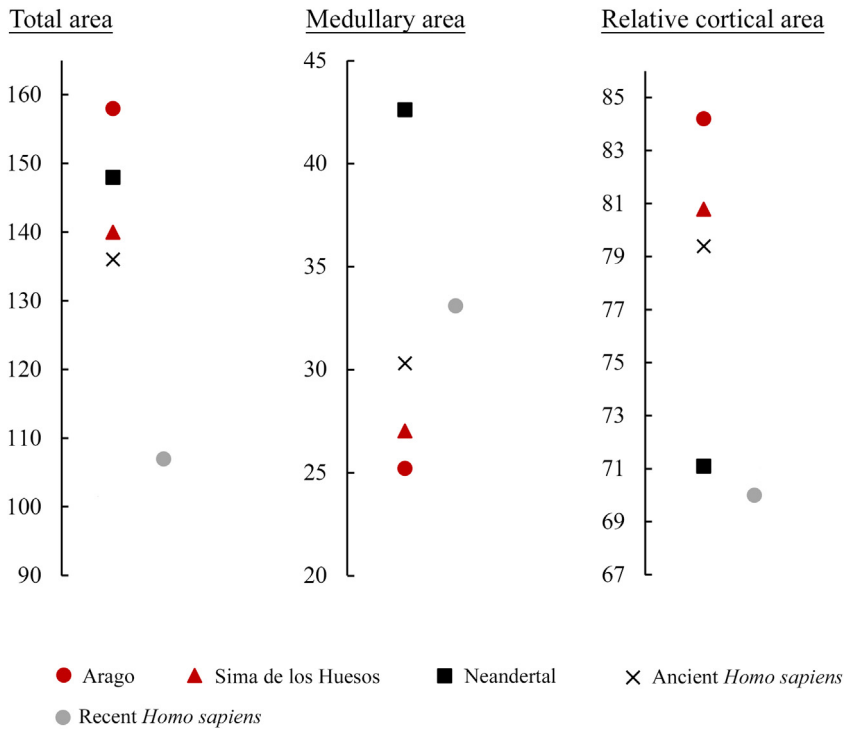

Fig. 8. Fibular cross-sectional geometric properties at midshaft: hominin fossils (mean values). See units in legend Table 3.
Propriétés géométriques des sections transversales du tibia : les hominines fossiles (valeurs moyennes). Voir les unités dans la légende du Tableau 3.

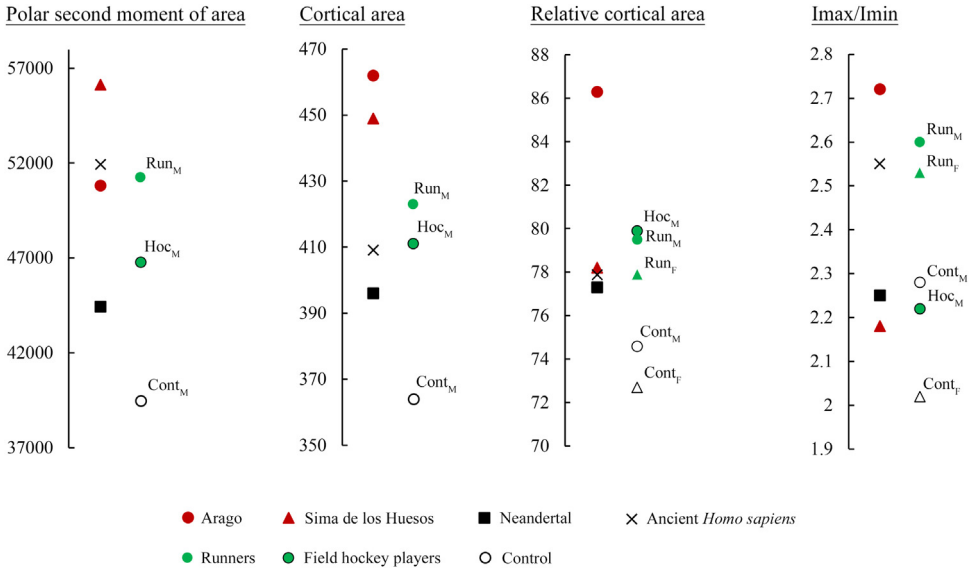

Fig. 9. Tibial cross-sectional geometric properties at midshaft: hominin fossils *versus* athletes (runners and field hockey players) (mean values). The control group includes non-athletes. See units in legend Table 3.
Propriétés géométriques des sections transversales du tibia à mi-diaphyse : hominines fossiles versus *athlètes (coureurs à pied et joueurs de hockey sur gazon) (valeurs moyennes). Le groupe de contrôle est composé des non-athlètes. Voir les unités dans la légende du Tableau 3.*

Please cite this article in press as: Chevalier, T., de Lumley, M.-A., Lower limb bone structure of Middle Pleistocene hominins from the Caune de l'Arago (Tautavel, France): Evolutionary and

Table 8
Fibular cross-sectional geometric properties at midshaft: all samples. Mean and standard deviation (in brackets). Meaning of abbreviations and units in legend Table 3. All data are from this study, excepted Sima, field hockey players, runner and control from Marchi and Shaw (2011) and Rodríguez et al. (2018).
Propriétés géométriques des sections transversales de la fibula : tous les échantillons. Moyennes et écarts-types (entre parenthèses). Voir la signification des abréviations et les unités dans la légende du Tableau 3. Toutes les données sont de cette étude, excepté celles de la Sima, des joueurs de hockey sur gazon et du groupe de contrôle qui proviennent de Marchi et Shaw (2011) et Rodríguez et al. (2018).

	N	J	TA	CA	TA-CA	%CA	Ix/Iy	Imax/Imin
50%								
Arago	5	4274 (521)	158 (10)	133 (5)	25.2 (5.5)	84.2 (2.7)	0.84 (0.17)	1.73 (0.22)
Sima de los Huesos	4	3283 (1147)	140 (24)	113 (20)	27.0 (6.6)	80.8 (3.6)	0.93[a] (0.13)	1.70 (0.26)
Neandertal	1	3340	148	105	42.6	71.1	0.47	2.11
Ancient *Homo sapiens*	4	3993 (1782)	136 (43)	109 (23)	30.3 (18.9)	79.4 (7.5)		
Recent *Homo sapiens* 50%	24–38	1872 (598)	107 (21)	73.5 (13.0)	33.1 (15.7)	70.0 (9.7)	1.34 (0.40)	1.79 (0.48)
Recent *Homo sapiens* 60%	24–38	1751 (579)	97.9 (21.6)	71 (12.1)	29.4 (14.4)	72.1 (9.5)	1.51 (0.53)	2.04 (0.71)
Field Hockey	17	2808 (720)		101 (10)			1.87	2.22 (0.77)
Runner	15	2507 (834)		95.2 (15.4)			1.96	2.39 (0.89)
Control	21	2207 (642)		89.5 (14.0)			1.74	2.21 (0.98)

[a] This index was calculated after reorienting the cross-sections of the Sima de los Huesos fibulas. The original mean and standard deviation are 1.13 and 0.52, respectively.

laterally at 65% (with a relatively high medial value), medial, posterior and lateral at 50% and medial and lateral at 35%. Thus, the maximal thickness in A141 runs medially and laterally along the diaphysis, as in *H. erectus* (as illustrated in Puymerail et al., 2012a, b), and cortical thickness is almost the same on all sides at midshaft (with the lowest value on the anterior side). Overall, the change in theta follows the change in the location of maximal cortical thickening (Fig. 12). Maximal cortical thickness in Sima (F-X) is medial at 80% (with a relatively high lateral value), medially and posteriorly at 65%, postero-medially at midshaft and almost posteriorly at 35%. Posterior cortical thickening at 35% is also well marked in F-XIII and F-IX (see above for more details on midshaft description). Thus, the maximal thickness in F-X is medial and turns anti-clockwise from the proximal to the distal part of this femur. This cortical thickening turns in the same way as the axis of maximal bending rigidity for which the angle of rotation is quantified with theta. This cortical "spiral" pattern is frequently observed in Neandertals (Chevalier et al., 2015; Chevalier and Lumley, 2018, 2022a). Clearly, the axis of maximal bending rigidity and the medial location of maximal cortical thickening in Sima (F-X) turn around the diaphysis more than in Arago (A141). Theta is from 42.6 to −48.1̊ in Sima and from 28.9̊ to −22.6̊ in Arago (Fig. 12). Note that the high proximal and lateral cortical thickness present in ancient *Homo* (*H. erectus*, Middle Pleistocene hominin, Neandertals) and associated with the buttressing running along the hypotrochanteric complex, is not possible to see here, as the cross-section located at about 75% cannot be observed (Chevalier et al., 2015; Chevalier and Lumley, 2018, 2022a; Puymerail et al., 2012a, b).

The Arago tibia (A120) presents a posterior bulge, or "pilaster", along the diaphysis (Fig. 13). This is clearly noticeable on the midshaft cross-section. It corresponds to posteromedial strengthening marked by cortical thickening. This morphology can also be described as a well-defined posteromedial border. The tibia AT-848 and TIB-III from Sima seem to share the same characteristic (Fig. 13). This feature is potentially analogous to the posterior pilaster. Such pilaster is uncommon in recent *H. sapiens*, but frequent in Upper Palaeolithic individuals (Trinkaus et al., 2022) and Neandertals (e.g., La Ferrassie 1, Amud 1, Chapelle-aux-Saints), although it may be only present on the proximal part of the diaphysis. From the cross-sections of Sima illustrated in Rodríguez et al. (2018), we cannot determine whether the tibiaes, which do not have an obvious pilaster at midshaft, have it in the proximal part (e.g., TIB-VI). However, this feature in Arago and in Sima (from published cross-sections)

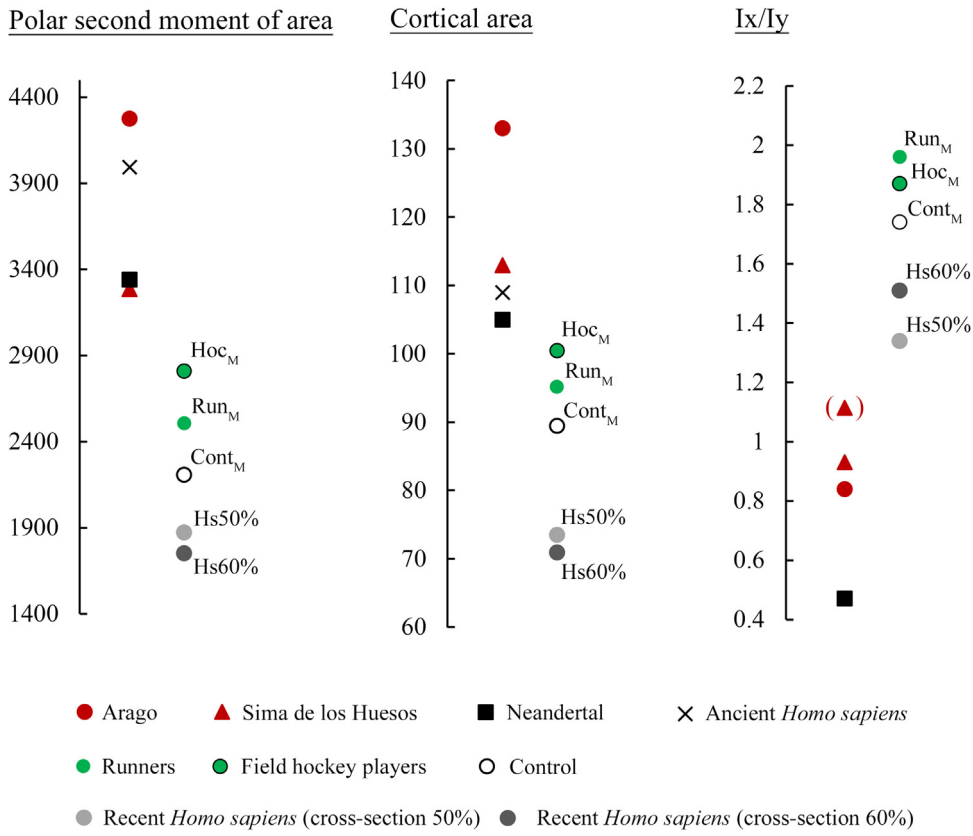

Fig. 10. Fibular cross-sectional geometric properties at midshaft: hominin fossils *versus* athletes (runners and field hockey players) (mean values). The control group includes non-athletes. See units in legend Table 3.
Propriétés géométriques des sections transversales de la fibula à mi-diaphyse : hominines fossiles versus *athlètes (coureurs à pied et joueurs de hockey sur gazon) (valeurs moyennes). Le groupe de contrôle est composé des non-athlètes. Voir les unités dans la légende du Tableau 3.*

seems to be more similar to a well-defined and large border than a pilaster, which appears very salient and narrow in Neandertals and Upper Palaeolithic tibias (Fig. 13).

Tibial borders are smooth and the faces are convex or flat in Arago and Sima, as in Neandertals (Fig. 13). This pattern differs from Upper Palaeolithic individuals for which the anterolateral face is often excavated (e.g., Caviglione, Cro-Magnon) and more marked proximally at about 65% where the interosseous line can be salient.

Fibular cross-sections in Arago and Sima show strong posterolateral cortical thickening which seems to be frequent in Upper Palaeolithic and Neolithic individuals (*analysis in progress*), but not in recent *H. sapiens* (Fig. 14). The medial border appears more salient in Arago than in Sima. Furthermore, the distance between the anterior border and the osseous crest is weak in Arago, in comparison to FIB-I and FIB-II in Sima (Fig. 14). This aspect in Arago is remarkable all along the proximal half of the diaphysis. In the more proximal part, the anterior border and the osseous crest form only one "anterior border" in Arago. In other words, it is difficult to differentiate these two anatomical features. The diaphysis is clearly strengthened given the mediolateral axis (approximatively). The fibulas from Arago do not present the anterior strengthening observed in some recent and ancient *H. sapiens*, like Cro-Magnon (Fig. 14). More precisely, at about 65% of bone length, the special "anterior border" in

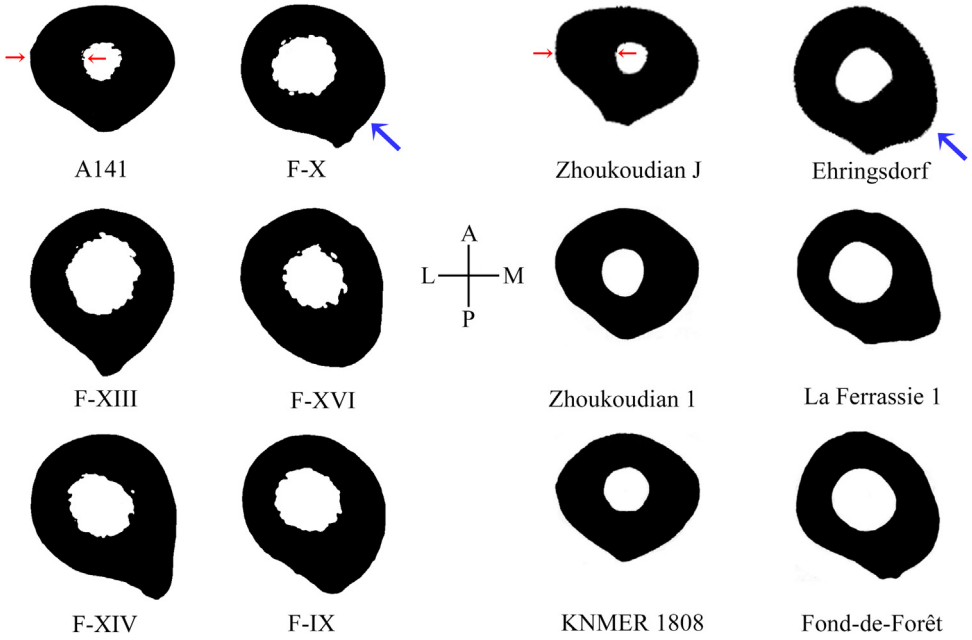

Fig. 11. Femoral cross-sections in Arago and Sima *versus Homo erectus* and Neandertal. The red arrows show the relatively high lateral cortical bone thickness found in Arago and *H. erectus* in contrast to the Sima and Neandertal pattern; the blue arrows show the posteromedial cortical thickening found in Sima and Neandertals. Arago: A141; Sima de los Huesos: F-X, IX, XIII, XIV, XVI; *H. erectus*: Zhoukoudian J, 1, KNMER 1808; Neandertals: Ehringsdorf, La Ferrassie 1, Fond-de-Forêt. Cross-sections are modified from Weidenreich (1938); Trinkaus and Ruff (1989); Ruff et al. (1993); Trinkaus (1997); Ruff (2008); Rodríguez et al. (2018); except A141 and Ehringsdorf from this study. All cross-sections are presented with the same breadth and orientation, and mirrored if necessary.
Sections transversales des fémurs de l'Arago et de la Sima versus Homo erectus *et Néandertal. La flèche rouge montre l'épaisseur de l'os cortical relativement élevée latéralement, identifiée à l'Arago et chez des* H. erectus*, contrastant avec le modèle néandertalien identifié à la Sima; la flèche bleue indique l'épaississement cortical postéro-médial trouvé à la Sima et chez les Néandertaliens. Arago : A141 ; Sima de los Huesos : F-X, IX, XIII, XIV, XVI ;* H. erectus *: Zhoukoudian J, 1, KNMER 1808 ; Néandertaliens : Ehringsdorf, La Ferrassie 1, Fond-de-Forêt. Les sections transversales sont modifiées d'après Weidenreich (1938); Trinkaus et Ruff (1989); Ruff et al. (1993) ; Trinkaus (1997) ; Ruff (2008); Rodríguez et al. (2018) ; excepté pour A141 et Ehringsdorf issues de cette étude. Toutes les sections transversales sont présentées avec les mêmes largeur et orientation. La latéralité a été inversée si nécessaire.*

Arago is salient but not very marked like in Cro-Magnon 4334. In addition, the strengthening in Arago only concerns this border and not the overall cross-section as in Cro-Magnon 4335.

5. Discussion

The concomitance of femurs, tibias and fibulas in the same prehistoric site is exceptional in the Middle Pleistocene. In this regard, the Caune de l'Arago and Sima de los Huesos sites are remarkable and the comparison of their lower long bones is determinant for characterizing the European Pleistocene evolutionary history and mobility levels and patterns. We sought here to determine whether the lower limb bones from Sima were closer to Neandertal than Arago, and whether individuals from both sites shared a (very) high level of mobility with probable displacements on uneven terrain or mountainous areas.

Overall, we have shown that the cross-sectional shapes of the lower limb bones from Arago and Sima hominins are close, if we consider mean comparisons or some individuals separately. At midshaft, we note the absence of the femoral pilaster (frequent in ancient *H. sapiens*), the presence of the tibial posterior pilaster and marked fibular posterolateral cortical thickening. Also, Arago, Sima

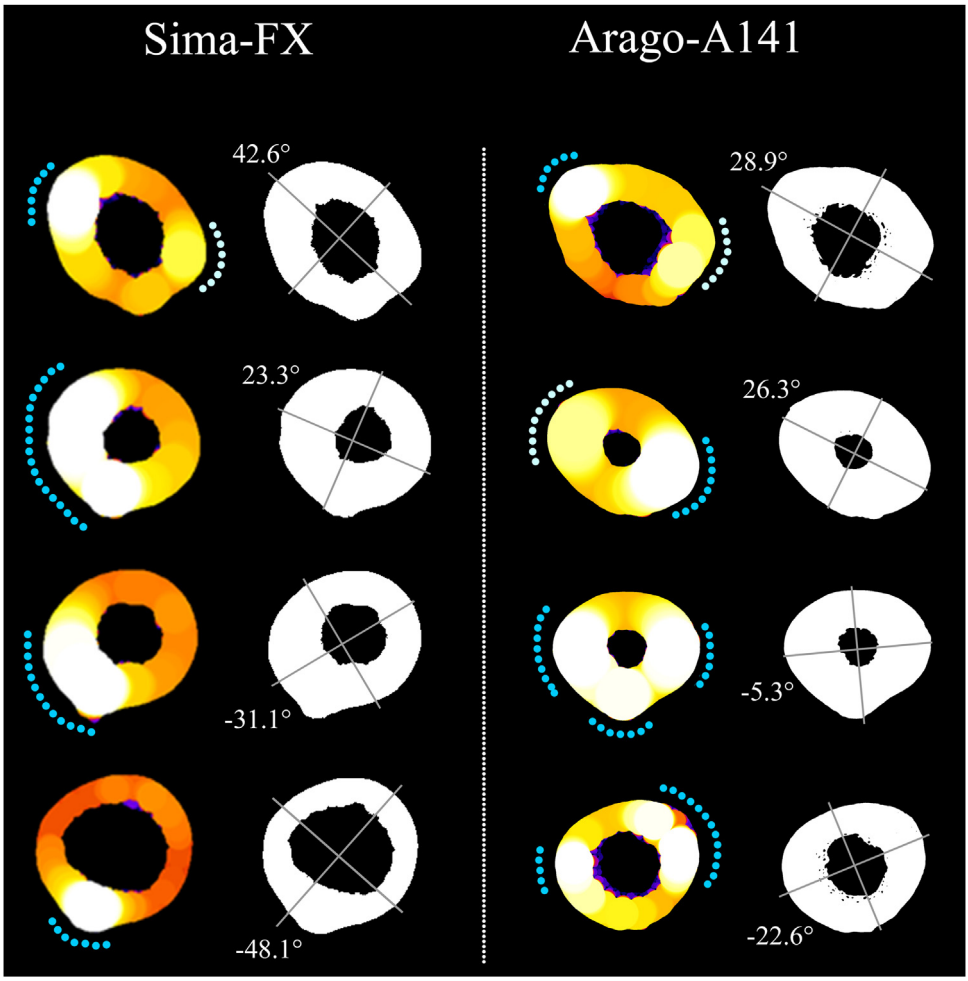

Fig. 12. Femoral cortical thickness and axis of maximal bending rigidity. The relative cortical thickness (i.e., cortical distribution) in each cross-section is highlighted with mapping (white: greatest thickness; red/purple: lowest thickness). The maximal thickness is also indicated with the dotted curved lines (deep blue: greatest thickness; light blue: high but not maximal thickness). We duplicated the cross-sections to present the minimum and maximum axis of bending rigidity, and the angle of the latter (theta, in degrees). A141 was horizontally flipped. Cross-section orientation: anterior is upward, medial is towards the left.

Épaisseur corticale du fémur et axe de rigidité à la flexion maximale. L'épaisseur corticale du fémur et sa distribution pour chaque section transversale sont mises en exergue par une cartographie (blanc : épaisseur la plus élevée ; rouge/violet : épaisseur la plus faible). L'épaisseur maximale est également soulignée par une ligne pointillée courbe (bleu foncé : épaisseur la plus élevée ; bleu clair : épaisseur élevée, mais pas la plus forte). Nous avons dupliqué les sections pour présenter les axes de rigidité à la flexion minimale et maximale, ainsi que l'angle pour l'axe de rigidité maximale (thêta, en degré). Les sections de A141 ont été symétrisées horizontalement. Orientation des sections : la face antérieure est dirigée vers le haut, la face médiale vers la gauche.

and Neandertals present large femoral diaphyseal size, in contrast to Trinil, Zhoukoudian and Lazaret, and a high relative cortical area (like Zhoukoudian) in contrast to Trinil and Lazaret.

However, various characteristics differentiates Arago from Sima and liken it to femurs from Zhoukoudian: femoral cortical distribution, and the femoral, tibial and fibular medullary area and relative cortical area. First, as expected, the femoral structural pattern at midshaft in Sima is close to the Neandertal pattern, with posteromedial cortical reinforcement. It differs from the Arago pattern, which is more closely related to *H. erectus*, with a more homogeneous distribution of cortical bone.

Please cite this article in press as: Chevalier, T., de Lumley, M.-A., Lower limb bone structure of Middle Pleistocene hominins from the Caune de l'Arago (Tautavel, France): Evolutionary and

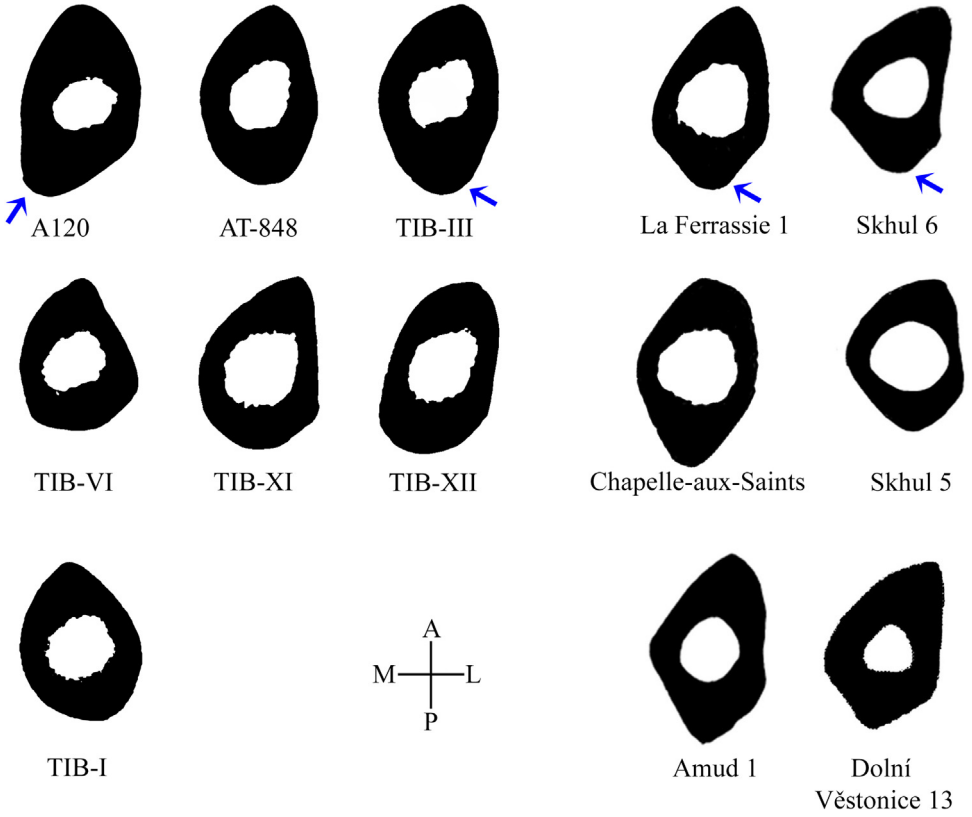

Fig. 13. Tibial cross-sections in Arago and Sima *versus* Neandertal and ancient *Homo sapiens*. We present some Neandertals and ancient *H. sapiens* with a clear posterior pilaster on midshaft cross-sections. The blue arrows show the posterior pilaster frequently observed in Middle Pleistocene hominins, Neandertals and ancient *H. sapiens*. Arago: A120; Sima de los Huesos: AT-848, Tib-I, III, VI, XI, XII; Neandertals: La Ferrassie 1, La Chapelle-aux-Saints, Amud 1; ancient *H. sapiens*: Skhul 5, 6, Dolní Věstonice 13. Cross-sections are modified from Trinkaus and Ruff (1999); Trinkaus (2006); Rodríguez et al. (2018); except A120, La Ferrassie 1, La Chapelle-aux-Saints from this study. All cross-sections are presented with the same breadth and orientation, and mirrored if necessary.
Sections transversales du tibia de l'Arago et de la Sima versus *Néandertal et les* Homo sapiens *anciens. Nous présentons quelques Néandertaliens et* H. sapiens *anciens pour lesquels la présence du pilastre postérieur est évidente à partir de la section transversale mi-diaphysaire. La flèche bleue montre le pilastre postérieur fréquemment observé chez les Hommes du Pléistocène moyen, Néandertaliens et* H. sapiens *anciens. Arago : A120 ; Sima de los Huesos : AT-848, Tib-I, III, VI, XI, XII ; Néandertaliens : La Ferrassie 1, La Chapelle-aux-Saints, Amud 1 ; anciens* H. sapiens *: Skhul 5, 6, Dolní Věstonice 13. Les sections transversales sont modifiées d'après Trinkaus et Ruff (1999) ; Trinkaus (2006) ; Rodríguez et al. (2018) ; excepté A120, La Ferrassie 1 et La Chapelle-aux-Saints qui proviennent de cette étude. Toutes les sections transversales sont présentées avec les mêmes largeur et orientation. La latéralité a été inversée si nécessaire.*

This femoral characteristic in Arago, associated with its cross-contour, contributes to its low relative bending rigidity (Ix/Iy), like for Zhoukoudian. The femoral Ix/Iy of Sima is similar to Neandertal, or intermediate between Arago and Neandertals, given the diaphyseal location. Secondly, the medullary areas are very low, and the relative cortical areas are very high in all lower limb bones in Arago (and close to the femurs from Zhoukoudian). Thus, when the Arago bones differ from those of Sima, they are closer to Zhoukoudian, and considering the same variables, Sima is closer to Neandertals.

Finally, femoral cross-sections at midshaft seem to show some clear distinctions between Arago and Sima, while tibial and fibular cross-sections reveal strong affinities. Furthermore, ancient

Please cite this article in press as: Chevalier, T., de Lumley, M.-A., Lower limb bone structure of Middle Pleistocene hominins from the Caune de l'Arago (Tautavel, France): Evolutionary and

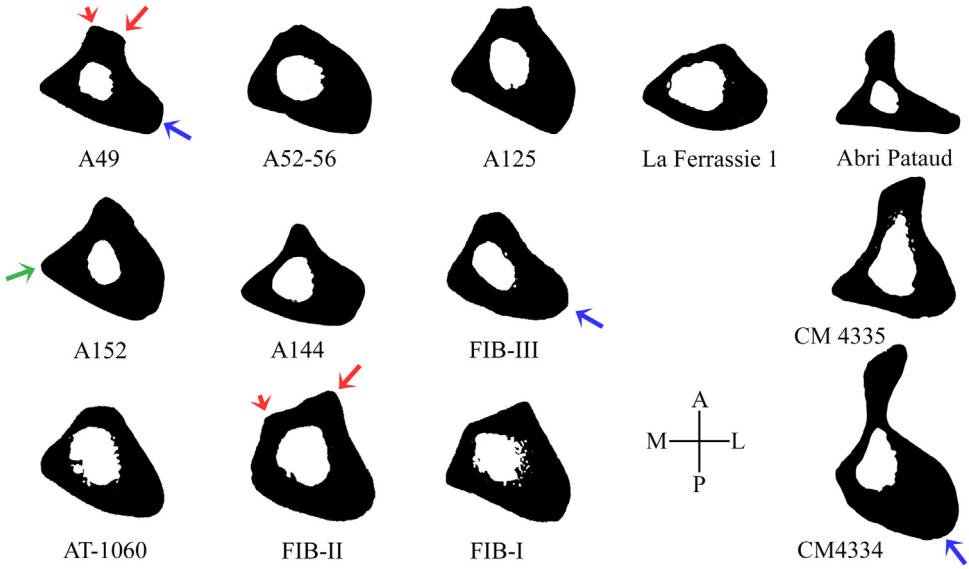

Fig. 14. Fibular cross-sections in Arago and Sima *versus* Neandertal and ancient *Homo sapiens*. The posterolateral buttressing (i.e., cortical bone thickening) is frequently present in Arago, Sima and some ancient *Homo sapiens*, and rare in recent *H. sapiens*. The blue arrows show the posterolateral buttressing; the red and great arrows show the anterior border; the red and small arrows show the interosseous crest; the green arrow shows the medial border. Sima de los Huesos fibulas are oriented differently than in Rodríguez et al. (2018). Arago: A49, A52-A56, A125, A144, A152; Sima de los Huesos: FIB-I, II, III, AT-1060; Neandertal: La Ferrassie 1; ancient *H. sapiens*: Cro-Magnon 4334, 4335, Pataud. All cross-sections are presented with the same breadth and orientation, and mirrored if necessary.
Sections transversales des fibulas de l'Arago et de la Sima versus *Néandertal et les* Homo sapiens *anciens. Le contrefort postérolatéral (c.-à-d., l'épaississement de l'os cortical) est fréquemment présent à l'Arago et à la Sima, et chez certains* Homo sapiens *anciens, et rarement chez les* H. sapiens *récents. Les flèches bleues montrent le contrefort postérolatéral ; les flèches rouges et grandes montrent le bord antérieur ; les flèches rouges et petites montrent la crête interosseuse ; la flèche verte montre le bord médial. Les fibulas de la Sima de los Huesos sont orientées différemment que dans l'étude de Rodríguez et al. (2018). Arago : A49, A52-A56, A125, A144, A152 ; Sima de los Huesos : FIB-I, II, III, AT-1060 ; Néandertalien : La Ferrassie 1 ; anciens* H. sapiens *: Cro-Magnon 4334, 4335, Pataud. Toutes les sections transversales sont présentées avec les mêmes largeur et orientation. La latéralité a été inversée si nécessaire.*

H. sapiens differ from Arago/*H. erectus* and Sima/Neandertal at femoral midshaft, but share leg structural patterns with these groups (e.g., the tibial posterior pilaster). Consequently, the relationship established between the femoral cross-sectional pattern and the pelvofemoral complex (Ruff, 1995; Ruff and Hayes, 1983a), and the one established between the physical activity and the structure of leg bones (tibia and fibula) (Marchi and Shaw, 2011; Shaw and Stock, 2009a) need to be discussed with regard to Arago and Sima bone structures.

5.1. Evolutionary affinities from the femoral pattern of bone cortical distribution

Bone structure depends on multiple factors, such as genetic and hormonal factors (Lovejoy et al., 2003; Pearson and Lieberman, 2004; Wallace et al., 2014), physical activity (Ruff et al., 2006; Shaw and Ryan, 2012; Shaw and Stock, 2009a, b; Trinkaus et al., 1994; Warden et al., 2014) and body shape and size (Ruff, 1995, 2000; Ruff et al., 1993). Interestingly, diaphyseal structural organization may be specific to a species or an evolutionary context regarding the femoral proximal and midshaft cross-sections (Ruff, 1995; Trinkaus and Ruff, 2012) and can help to clarify taxonomical affinities in *Homo* (Chevalier et al., 2015; Puymerail et al., 2012a; Ruff et al., 2015a).

Based on a mechanical model, Ruff (1995) highlighted the effects of biacetabular breadth and femoral neck length on the proximal femoral diaphysis. A wide pelvis and long neck tend to increase

the relative medio-lateral bending strength of the femoral diaphysis. This is the main hypothesis put foward to explain the specific femoral shape diaphysis of *H. erectus* marked by anteroposterior flattening, or inversely mediolateral broadening. Femoral flattening (i.e., low Ix/Iy) in *H. erectus* is also present at midshaft and would be influenced by the pelvofemoral complex (Ruff, 1995). Some analyses in Pearson et al. (2014) (but not all) emphasize the significant correlation of bi-iliac breadth and "body shape" (bi-iliac breadth divided by femoral length) with femoral midshaft shape (Imax/Imin or pilastric index). The femurs from Arago and Sima also present a low shape index (Ix/Iy) and do not present a femoral pilaster. The presence of a pilaster has been related to a high level of mobility (Holt, 2003; Shackelford, 2007) and the midshaft shape is considered to be a viable and valuable means of exploring mobility, despite questions about the influence of body proportions (Shaw and Stock, 2011). However, the absence of the pilaster and the presence of a flat diaphysis were not interpreted in early *Homo* as an adaptation of the bone to a low level of mobility. A structural compromise because of mediolateral and anteroposterior strains, due to the pelvofemoral complex morphology and bending related to bipedal mobility, could be at the origin of certain structures without pilasters and low Ix/Iy.

Additionally, femoral cortical distribution at midshaft is distinct in *H. erectus*, *Homo neanderthalensis* and ancient *H. sapiens* (data summarized in Chevalier et al., 2015; Chevalier and Lumley, 2018, 2022a; Trinkaus and Ruff, 2012). Ancient *Homo* (from putative *Homo habilis* to Neandertal) presents a medial buttress, i.e., medial cortical reinforcement (Kennedy, 1985; Trinkaus and Ruff, 2012). This kind of cortical bone reinforcement can be better defined by mapping cortical bone distribution along the diaphysis (See Chevalier et al., 2015; Puymerail et al., 2012a). This reinforcement is distinct in Neandertals. It runs medially and obliquely along the diaphysis from the proximal to the middle diaphyseal portion in some Neandertals (Puymerail et al., 2012b, 2013). From cross-sections, Chevalier et al. (2015) and Chevalier and Lumley (2018) identified a frequent strong midshaft posteromedial reinforcement of the cortical thickness in Neandertals and some Middle Pleistocene hominins. Here, we confirm the presence of such a pattern in Sima (and not in Arago). It results from the medial spiral distribution pattern of diaphyseal maximal cortical thickness (Chevalier et al., 2015). This spiral originates on the proximal and medial diaphyseal region and ends approximately at mid-diaphysis on the posteromedial region. Thus, we can differentiate the *H. erectus* medial buttress, associated with straight medial reinforcement (Puymerail et al., 2012a), to the Neandertal posteromedial buttress, associated with an oblique reinforcement, also called spiral reinforcement (Chevalier et al., 2015; Chevalier and Lumley, 2018), and with posterior cortical thickening associated with the pilaster of ancient *H. sapiens* (Chevalier and Lumley, 2022a; Mednikova and Trinkaus, 2001; Trinkaus, 1997, 2006; Trinkaus and Ruff, 1999).

To a certain extent, the posteromedial reinforcement is a classical feature, indirectly observed in *Homo* (see Ruff and Hayes, 1983a), unlike marked posteromedial cortical thickening. The position of the femoral head (i.e., anterior offset) and the curvature of the femur in *H. sapiens* generate an axis of maximal bending stress that rotates down the shaft with a roughly mediolateral orientation proximally to an anteroposterior orientation distally (Ruff, 1981; Ruff and Hayes, 1983a). Thus, maximal bending stress (i.e., axis of maximal bending rigidity) at midshaft goes through the posteromedial side (see figure 6 in Ruff and Hayes, 1983a), where we observed marked cortical thickening in Sima and Neandertals (Fig. 12). The overall characteristics of the pelvofemoral complex (e.g., biacetabular breadth, long femoral neck, femoral anteversion angle, collo-diaphyseal angle, and also femoral curvature) would be the main factors constituting the general structural pattern of the femoral diaphysis (Ruff, 1995; Ruff et al., 2006; Ruff and Hayes, 1983a). The observation and mechanical explanations of Ruff and Hayes (1983a) do not require maximum cortical thickness to be in the axis of greatest rigidity and in a site-specific location, but it can be expected that strong cortical thickening (if any) will be approximately in this axis. The variables involved in the model of the latter authors are relevant to explain what we observed in our fossil samples. Consequently, the femur is not only modelled by mobility throughout life. Particular pelvofemoral conditions would have generated specific femoral cross-sectional shape and cortical distribution in ancient *Homo*, such the posteromedial buttressing at midshaft frequently observed in Sima and Neandertals. The structural pattern of Arago is also influenced by the same variables, but probably not by the same value for each variable. If we hypothesize that the common pelvofemoral complex would be mainly driven by

Please cite this article in press as: Chevalier, T., de Lumley, M.-A., Lower limb bone structure of Middle Pleistocene hominins from the Caune de l'Arago (Tautavel, France): Evolutionary and

genetic factors, and not by physical activity, then the femoral diaphyseal cortical pattern would be a good indicator of evolutionary affinities. Thus, our analysis of Arago and Sima would confirm previous observations on cranial and postcranial bones from Sima highlighting many Neandertal-derived features in Sima (Arsuaga et al., 2015; Bermúdez de Castro et al., 2018), while Arago shows plesiomorphic features (Arsuaga et al., 2015; Lumley, 2015). However, we do not exclude the influence of mobility (or body size) on marked localized cortical thickening. Consequently, we suggest that (1) the usual pelvofemoral complex frequently observed in *Homo* would generate a usual human pattern of relative bending rigidity/strength along the diaphysis (related to the shape of the diaphysis cross-sections), (2) some particular conditions of the pelvofemoral complex (with possible consequences for the variation of the angle of maximal bending rigidity along the diaphysis) would be at the origin of the singular pattern of cortical distribution (as in Neandertal), or singular cross-sectional shape (as in *H. erectus*), and (3) site-specific cortical thickening could be increasingly marked with high levels of mobility (or body mass).

5.2. Behavioural affinities from tibial and fibular shapes

The femur is the most frequently found lower limb bones in the Early and Middle Pleistocene of Asia, Africa and Europe, and specifically in key areas, such as West and East Turkana (Kenya), Zhoukoudian (China), Trinil (Indonesia), Sima (Spain) and Arago (France). The femoral diaphyseal is impacted by the level and pattern of mobility (e.g., Holt, 2003; Shackelford, 2007; Sparacello et al., 2014; Sparacello and Marchi, 2008; Stock, 2006; Ruff, 1999; Ruff et al., 2015b), but the structure of the diaphysis is influenced by the pelvo-femoral complex (as seen above; Ruff, 1995; Ruff et al., 2006; Ruff and Hayes, 1983a). Some authors have noted conflicting results in inferring mobility from femoral and tibial shape at midshaft (Holt, 2003; Ruff et al., 2006). Variations in the level and pattern of locomotor activity, and notably activity in different ontogenetic stages, and variations in impact level and frequency, may have generated variate bone adaptation (see discussion in Pearson et al., 2014, and references therein). Note also that femoral mid-diaphyseal shape is influenced by femoral length, and the more mobile populations are, the more this factor could influence femoral diaphyseal shape (Sparacello et al., 2018). This relationship was not observed for the tibia. Like the femur, the tibia of Pleistocene hominins has been studied from a functional perspective (Holt, 2003; Lovejoy and Trinkaus, 1980; Trinkaus and Ruff, 1999; Ruff et al., 2015b; Sparacello et al., 2018). Such analyses are supported by bone studies of athletes showing the impact of specific activity on tibial structure (Nikander et al., 2010; Rantalainen et al., 2015; Shaw and Stock, 2009a; Weatherholt and Warden, 2016; Wilks et al., 2009). In contrast, fibular cross-sectional geometry has been little studied in past populations. The fact that the fibula is a low weight-bearing bone (Funk et al., 2004; Goh et al., 1992; Lambert, 1971; Takebe et al., 1984; Wang et al., 1996) and its scant presence in ancient periods probably explain the low interest it has generated (Marchi, 2007). However, studies on primates (Marchi, 2007, 2015), athletes (Hart et al., 2020; Lüscher et al., 2019; Marchi and Shaw, 2011), early *Homo* (Marchi et al., 2019) and Upper Palaeolithic and Holocene groups (Sparacello et al., 2014, 2018) highlight the importance of including fibular cross-sectional geometry in locomotor analysis. Indeed, the weight-bearing contribution varies depending on foot movement (i.e., ankle position) (Goh et al., 1992; Takebe et al., 1984; Thomas et al., 1995; Wang et al., 1996) and induces changes in mechanical loads generating bone modelling to adapt the fibular structure to preserve its integrity.

In this regard, the European Middle Pleistocene was particularly remarkable with the presence of tibias and fibulas in Arago and Sima, in addition to femurs (Arsuaga et al., 2015; Carretero et al., 2012; Chevalier and Lumley, 2022a, b, c; Lovejoy, 1982; Lumley and Lamy, 1982; Rodríguez et al., 2018). In our study, the most relevant mechanical parameters for comparing Arago, Sima and athletes in order to infer the pattern and level of mobility are the "shape" of tibias and fibulas studied from biomechanical parameters (Ix/Iy, Imax/Imin) and cross-contours. The Arago tibia (A120), like ancient *H. sapiens*, presents relative bending rigidity (Imax/Imin) close to that of runners, while the means of the Sima tibias are close to those of field hockey players. However, we have only one tibia in Arago. Three out of the seven tibias in Sima (studied in Rodríguez et al., 2018) also yield values close to those of runners. Thus, the tibial shape of several Middle Pleistocene European individuals is similar to that of runners, and greatly differs from non-athletic individuals. The intense practice of runners involved

Please cite this article in press as: Chevalier, T., de Lumley, M.-A., Lower limb bone structure of Middle Pleistocene hominins from the Caune de l'Arago (Tautavel, France): Evolutionary and

in a preferential unidirectional pattern of mobility has modified their diaphysis by strengthening it anteroposteriorly, approximately. The tibial posterior "pilaster" in some Arago and Sima individuals contributes to their high Imax/Imin values, but we do not know if athletes present the same pilaster. Note that the posterior pilaster is not present in the immature tibia of Arago (A95-A96, Chevalier, 2022; Chevalier and Lumley, 2022b). In Shaw and Stock (2009a), the tibial shape of runners and field hockey players differs significantly, but none of them are significantly different to non-athletes. Thus, tibial shape is a means of differentiating intense and radically distinct locomotor practices (i.e., unidirectional *versus* multidirectional locomotor pattern). In this regard, we can assume that running was commonly practised by Middle Pleistocene hominins.

In contrast, tibial cross-contours with flat or convex sides in Sima, Arago and Neandertals could be explained by a multidirectional locomotor pattern. However, some doubts arise given the very high Imax/Imin resulting from to unidirectional locomotor pattern. We can suggest that (1) there would be a distinct musculoskeletal development between Pleistocene hominins/Neandertal and *H. sapiens*, which it is difficult to prove without strong evidence, (2) the pelvofemoral complex (e.g., wide pelvis) would have influenced tibial shape although it is only expected to strongly influence the femur (Pearson et al., 2014; Ruff et al., 2006), or (3) tibia shape would reflect the result of two distinct locomotor patterns or changes in locomotor pattern during growth (with structural retention of early locomotor pattern). This latter suggestion is supported in Arago by the distinction and similitude between the tibial cross-section of the immature individual A95-A96 and adult A120. Both tibias have the same overall structural pattern marked by a clear posteromedial border (while stronger in A120) associated with cortical thickening (Chevalier, 2022). However, A95-A96 unexpectedly presents a very rounded cross-section for the human tibia regardless of the age of the individual. This structural pattern drastically contrasts with the very high anteroposterior elongation of A120, which could be due to the unidirectional locomotor pattern, although the A95-A96 pattern could be due to a multidirectional locomotor pattern (and a specific developmental pattern, suggestion 1). Two distinct patterns of mobility, marked by intensive practice, could possibly have existed, and would differentiate the immature individual of about 10 years (A95-A96) from the adult (A120). However, evidence is still lacking to relate such rounding of the Arago tibia A95-A96 to functional patterns. Whether or not we accept the multidirectional hypothesis in the younger individual, such a distinction between A120 and A95-A96, despite a similar overall pattern, reinforces the hypothesis of a high level of mobility in A120 and drastic change during growth.

Finally, it raises questions about the analogy of the posterolateral border in Arago with the posterior pilaster observed in Neandertal and Upper Palaeolithic individuals, the genetic origin of this feature and the impact of unknown tibial torsion. Note that we do not classify the posterolateral border of A95-A96 as a posterior pilaster as it is not as prominent as A120.

No significant distinction in fibular shape was observed between athletes and nonathletes, nor between runners and field hockey players (Marchi and Shaw, 2011). On account of this result, it is difficult to functionally interpret the shape indices (Ix/Iy) in Arago and Sima, which present very low values (means range: 0.84–0.93) in comparison to the sample of Marchi and Shaw (mean range: 1.74–1.96). Currently, it does not seem appropriate to put forward a functional explanation. Bone orientation could have strongly influenced data when taking measurements. Indeed, Marchi and Shaw (2011) used data taken with pQCT on living humans (Shaw and Stock, 2009a), in contrast to our data taken on dry bone. Imax/Imin is a better index, but it does not provide information on the orientation of maximum rigidity. Comparisons of data acquired with the same method, are possible using the dry bone of recent *H. sapiens* (supposedly non-athletes). Finally, when we include both indices in our analysis, Imax/Imin in Arago and Sima is close to recent *H. sapiens*, but Ix/Iy is clearly distinct. Thus, the fibulas of Arago and Sima would have been subjected to high mediolateral stress, due to the eversion/inversion movement experienced in irregular/mountainous terrain. Such locomotor activity and ankle mobility transfer more weight to the fibula (Goh et al., 1992; Takebe et al., 1984; Thomas et al., 1995; Wang et al., 1996) and generate bone adaptation. Unfortunately, other fossil studies including discussions about the influence of the type of terrain and level of mobility do not integrate the fibular Ix/Iy index (Sparacello et al., 2014, 2018). In Chevalier (2022), two other indices are added: robusticity (polar second moment second of area standardized by bone length and body mass) and relative robusticity (the ratio of fibular and tibial relative polar second moment second of area) (see details in Chevalier, 2022; Chevalier and

Lumley, 2022c). The body masses associated with the fibulas were not known but a body mass of 80 kg was chosen to scale. This high body mass was estimated from the pelvis A44 (Ruff, 2010) and the femur A57 (Chevalier, 2022), and associated with the estimated fibular bone length of 364 mm (mean estimated bone length of A144 and A52-A56) (see details in Chevalier, 2022; Chevalier and Lumley, 2022c). The body mass and bone length used to scale are very high and high, respectively. Such values could underestimate the robusticity index. The fibulas used are A49, A52/A56, A125 and A144. All results are homogenous and highlight the very high robusticity of the fibula from Arago (much more so than athletes). Chevalier (2022) also compared the polar second moment of area of distinct fibulas to the tibia. It is not possible to confirm whether one of the fibulas belongs to the same individual as tibia A120 (stratigraphically certain bone associations are quite possible), but all results are homogenous and indicate very high relative fibular robusticity. These fibular robusticity indices are always impressive with regard to athletes (Chevalier, 2022), in the same way as for Upper Palaeolithic individuals from mountainous areas (Sparacello et al., 2014, 2018). Varied foot movements, as a result of frequent directional changes, favoured such fibular adaptation (Marchi et al., 2011; Marchi and Shaw, 2011; Sparacello et al., 2014). Field hockey players and humans crossing in irregular terrain, experienced the same overall locomotor pattern with multidirectional stress, but mountainous areas (i.e., areas with variations in elevation) with downhill and uphill engender higher stress generated by strong impact (Gottschall and Kram, 2005). Specifically, the fibula with eversion and dorsiflexion of the foot in rough and hilly/mountainous terrain experience maximal loads (Wang et al., 1996).

Consequently, hominins from Arago and Sima attained a very high level of mobility, with possible running and frequent movements across irregular terrain (this study; Chevalier, 2022; Rodríguez et al., 2018). The topography around Arago Cave with plains and semi-mountainous/hilly areas is consistent with this functional hypothesis. The very high values of some structural parameters in human fossil bones raise questions about the correlation between bone structure and the pattern and level of mobility. In other words, do the observed differences in bone structure accurately reflect (at the same level) differences in physical behaviour? We can also ask whether bone mechano-responsiveness was the same in past populations, and at what growth stage early humans became highly active during their lifetime, which has a strong influence on the bone's ability to adapt and on adult bone shape and robusticity.

5.3. Relative cortical area and functional inference

Among the distinctive traits of the Arago lower limb long bones, we note a high to very impressive relative cortical area, and low medullary area, in contrast to the Trinil and Lazaret hominins (and also *H. sapiens*). Many factors affecting bone modelling can induce change in relative cortical area, such as growth pattern, hormonal level, diet/living conditions, mechano-responsiveness of endosteal and periosteal surfaces, and aging (e.g., Birkhold et al., 2016; Garn, 1970; Garn et al., 1969; Kennedy, 1985; Ruff et al., 1994; Ruff and Hayes, 1983b). Here, we are only interested in the relationship that may exist between the relative cortical area and the level of mobility in the case of the exceptional values found in Arago. Generally, the relative cortical area is not considered relevant from a functional perspective, as it is difficult to interpret without consideration of other cross-sectional geometric properties, and because the cortical area needs to be scaled with body mass (Ruff, 1992b; Ruff et al., 1993, 1994, 2018). Indeed, the same relative cortical area can be acquired with different cortical distributions. Cortical thickness can be homogeneously distributed (see Arago, A141 at midshaft), vary all around the cross-section with the maximal thickness located in a specific side (see Sima, F-X at midshaft), and extend from the endosteal and periosteal surfaces. An increase in the relative cortical area can be due to an increase in the cortical area from the periosteal surface (with the same medullary area) or an increase in the cortical area with a reduction of the medullary area by bone formation on the endosteal surface (with the same total area). We deduced from the hypothetic model of Lazenby (1990) and van der Meulen et al. (2001) that the relative cortical area, or amount of cortical area, is not well-correlated with the geometrical parameters (e.g., second moment of area and section modulus) used to evaluate bone mechanical properties (e.g., bending rigidity and strength). However, for the same cross-sectional size (i.e., total area), the bone with the higher relative cortical area will be stronger. The high relative cortical area in Arago results in part from the maintenance or deposition of a large amount of endosteal bone. Lovejoy (1982) questioned the benefits of

Please cite this article in press as: Chevalier, T., de Lumley, M.-A., Lower limb bone structure of Middle Pleistocene hominins from the Caune de l'Arago (Tautavel, France): Evolutionary and

such a medullary reduction in Arago, knowing that for the same amount of cortical bone, an increase in the subperiosteal surface would have been more beneficial from a mechanical perspective. He considered that medullary reduction was not the best possible way to adapt, which was in contradiction with what was expected of bone adaptation according to Lanyon and Baggott (1976). However, Shaw and Stock (2009a) found significant differences in the tibial relative cortical area between athletes and non-athletes (but no difference between runners and field hockey players). Likewise, Warden et al. (2014) highlight the increase in the humeral total area and reduction in the medullary area of the dominant arm by comparisons of throwing-to-nonthrowing arms in professional baseball players. Thus, the high level of throwing activity increases the relative cortical area.

The functional hypothesis can also be discussed in the light of the structural characteristics of immature fossils, by taking into account relative cortical area and bone shape. First, Neandertal, Sima and Arago immature individuals present high relative cortical area (Chevalier and Lumley, 2022a, b, c; García-Gonzales et al., 2016; Ruff et al., 1994) suggesting that this trait could be genetically controlled or reflect other systemic factors (e.g., hormonal factors). Secondly, the young tibia A95-A96 presents a very low shape index (i.e., low Imax/Imin) compared to A120, which could imply that its diaphysis was not modelled as a result of high level of mobility. However, both present the same relative cortical area (86.3% *versus* 85.7%). Consequently, the high relative cortical area in A95-A96 would not be functional and the cortical thickening in the axis of greater bending rigidity in A120 would result from cortical redistribution to maintain bone integrity during high levels of mobility.

The study of the femur provides additional information based on the medullary area. The midshaft medullary area of the adult femur A141 is almost the same as that of A38, a femur from Arago belonging to an individual of about 10 years old (Chevalier and Lumley, 2022a), although the cross-section total area of A38 is half the size of A141. From mid-adolescence onwards, the mechanical responsiveness of the endosteal surface increases relatively to the periosteal surface and causes endosteal contraction if mechanical loading increases (Bass et al., 2002; Kontulainen et al., 2002; Ruff et al., 1994) even if it is not very beneficial mechanically (Lazenby, 1990; van der Meulen et al., 2001). Thus, the high level of activity in mid-adolescence may have stimulated endosteal formation and reduced endosteal resorption, resulting in the maintenance of the early adolescent medullary area.

Consequently, the high relative cortical area and small medullary area in lower limb bones from Arago could be interpreted as an endostructural signature of high levels of mobility combined with systemic effect, and as a result of a high maximal cortical thickness driven by the maximal axis of bending rigidity.

6. Conclusion

The lower limb bone structure of the Caune de l'Arago shares many characteristics with Middle Pleistocene hominins and Neandertals, like the Sima de los Huesos fossils. However, the femoral midshaft pattern in Sima is similar to that of Neandertal, in contrast to Arago, which is closer to *H. erectus*. These patterns depend on partially genetically controlled singular characteristics of the pelvofemoral complex and tend to confirm the previously revealed evolutionary affinities in cranial and postcranial bones, and teeth. The fibular and tibial cross-sectional geometry of Arago and Sima are functionally more informative. In comparisons to structural models of athletes, we observe that the leg bone structure in Arago is adapted to a high level of mobility and frequent and abrupt changes of direction, generating a substantial level of foot eversion/inversion. Considerable variation in ankle mobility also occurs when crossing irregular terrains and terrains with marked downhill and uphill slopes. This overall pattern and level of mobility attributed to Arago hominins was previously suggested for the Sima hominins. The mobility hypothesis for Arago hominins is consistent with the environment of Arago Cave and hominin hunting practices. It suggests intensive/frequent occupation of the surrounding plains and rugged terrain. Note that the structural pattern of the Arago tibia is compatible with running. Finally, additional data on the structural consequences of adaptive bone trade-off, when an individual has a very high level of mobility on flat terrains (with unidirectional locomotor pattern) and intensive movement on uneven or mountainous areas (with multidirectional locomotor pattern), could substantiate our conclusion regarding the concomitance of some structural features.

Please cite this article in press as: Chevalier, T., de Lumley, M.-A., Lower limb bone structure of Middle Pleistocene hominins from the Caune de l'Arago (Tautavel, France): Evolutionary and

Acknowledgements

We are grateful to Professor Henry de Lumley and to Anna Echassoux (IPH, Paris) for inviting us to participate to this special issue. We wish to thank Christian Perrenoud (UMR 7194 HNHP, MNHN), the current director of excavations at la Caune de l'Arago, and all those who have participated in the Arago excavations since 1964. Thanks to Jérôme Hosdez, research engineer at the ISIS4D X-ray platform (University of Lille, France), funded by the International Campus on Safety and Intermodality in Transportation (CISIT), the Haut-de-France Region, the European Community, and the National Centre for Scientific Research (CNRS); Marta Bellato (UMS 2700) and Miguel García-Sanz, technical supervisor and operator at AST-RX, plateforme d'Accès Scientifique à la Tomographie à Rayons X, UMS 2700 2AD Acquisition et Analyse de Données pour l'Histoire naturelle CNRS-Muséum National d'Histoire Naturelle (MNHN), Paris; Antoine Balzeau and Dominique Grimaud-Hervé (UMR 7194 HNHP, CNRS, MNHN) and Martin Friess (UMR 7206 Eco-Anthropologie, CNRS, MNHN) for access to the microcomputed tomography (micro-CT) scan archives of the MNHN (Paris, France); Sébastien Villotte (UMR 7206 Eco-Anthropologie, CNRS, MNHN, university of Paris) and Adrien Thibeault (PACEA, UMR 5199, university of Bordeaux) for sharing microtomography data, funded by ANR Gravett'os (ANR-15-CE33-0004), and Véronique Laborde (UMR 7206 Eco-Anthropologie, CNRS, MNHN, university of Paris) who prepared the bones for microtomography acquisitions; Denis Dainat (EPCC, Tautavel) for the photographs of the human remains of la Caune de l'Arago. We extend special thanks to Thomas Colard (PACEA, UMR 5199, university of Bordeaux; university of Lille), who participates in the organization of numerous scanning sessions at ISIS4D (University of Lille, France).

Microtomography acquisitions of the human remains from la Caune de l'Arago were funded by the Regional Service of Archaeology of the Occitania Region (SRA, Occitanie, France).

References

Arnold, L.J., Demuro, M., Parès, J.M., Arsuaga, J.L., Aranburu, A., Bermudez de Castro, J.M., Carbonell, E., 2014. Luminescence dating and palaeomagnetic age contrainst on hominins from Sima de los Huesos, Atapuerca, Spain. Journal of Human Evolution 67, 85–107.

Arsuaga, J.L., Carretero, J.M., Lorenzo, C., Gómez-Olivencia, A., García-González, R., Bonmatí, A., Quam, R.M., Pantoja-Pérez, A., Martínez, I., Aranburu, A., Gracia-Téllez, A., Poza-Rey, E., Sala, N., García, N., Sala, N., García, N., Alcázar de Velasco, A., Cuenca-Bescós, G., Bermúdez de Castro, J.M., Carbonell, E., 2015. Postcranial morphology of the middle Pleistocene humans from Sima de los Huesos, Spain. Proceeding of the National Academy of Sciences of the United States of America 112 (37), 11524–11529.

Arsuaga, J.L., Martínez, I., Arnold, L.J., Aranburu, A., Gracia-Téllez, A., Sharp, W.D., Quam, R.M., Falguères, C., Pantoja-Pérez, A., Bischoff, J., Poza-Rey, E., Parés, J.M., Carretero, J.M., Demuro, M., Lorenzo, C., Sala, N., Martinón-Torres, M., García, N., Alcázar de Velasco, A., Cuenca-Bescós, G., Gómez-Olivencia, A., Moreno, D., Pablos, A., Shen, C.-C., Rodríguez, L., Ortega, A.I., García, R., Bonmatí, A., Bermúdez de Castro, J.M., Carbonell, E., 2014. Neandertal roots: Cranial and chronological evidence from Sima de los Huesos, Atapuerca, Spain. Science 344 (6190), 1358–1363.

Bass, S.L., Saxon, L., Daly, R.M., Turner, C.H., Robling, A.G., Seeman, E., Stucckey, S., 2002. The effect of mechanical loading on the size and shape of bone in pre-, peri-, and postpubertal girls: a study in tennis players. Journal of Bone and Mineral Research 17 (12), 2274–2280.

Bermúdez de Castro, J.M., et al., 2018. Metric and morphological comparison between the Arago (France) and Atapuerca-Sima de los Huesos (Spain) dental samples, and the origin of Neanderthals. Quaternary Science Reviews 217, 45–61.

Birkhold, A.I., Razi, H., Duda, G.N., Weinkamer, R., Checa, S., Willie, B.M., 2016. The periosteal bone surface is less mechano-responsive than the endocortical. Scientific Reports 6, 23480.

Carretero, J.M., Rodríguez, L., García-Gonzáles, R., Arsuaga, J.L., Gómez-Olivencia, A., Lorenzo, C., Bonmatí, A., Gracia, A., Martínez, I., Quam, R., 2012. Stature estimation from complete long bones in Middle Pleistocene humans from the Sima de los Huesos, Sierra de Atapuerca (Spain). Journal of Human Evolution 62, 242–255.

Chevalier, T., 2022. Modèle structural des os longs de l'Homme de la Caune de l'Arago : interprétation et discussion. In: Lumley, M.-A. (Ed.), Les restes humains du Pléistocène moyen de la Caune de l'Arago. Caune de l'Arago. Tautavel-en-Roussillon, Pyrénées-Orientales, France, Tome IX, Chapitre 15. CNRS Éditions, Paris (*in press*).

Chevalier, T., Lumley, M.-A. de, 2018. Les fémurs Laz 13, Laz 15 et Laz 17, Laz 25 de la grotte du Lazaret. In: Lumley, M.-A. (Ed.), Les restes humains fossiles de la grotte du Lazaret, Nice, Alpes-Maritimes, France, Des *Homo erectus* européens évolués en voie de néandertalisation, Chapitre XV. CNRS Éditions, Paris, pp. 435–468.

Chevalier, T., Lumley, M.-A., 2022a. Le membre inférieur de l'Homme de la Caune de l'Arago. Les fémurs de l'Homme de la Caune de l'Arago (A17, A38, A48, A51, A53, A57, A141). In: Lumley, M.-A. de (Ed.), Les restes humains du Pléistocène moyen de la Caune de l'Arago. Caune de l'Arago. Tautavel-en-Roussillon, Pyrénées-Orientales, France, Tome IX, Chapitre 14 (14.1). CNRS Éditions, Paris (*in press a*).

Chevalier, T., Lumley, M.-A., 2022b. Le membre inférieur de l'Homme de la Caune de l'Arago. Les tibias de l'Homme de la Caune de l'Arago (A95-A96, A120). In: Lumley, M.-A. (Ed.), Les restes humains du Pléistocène moyen de la Caune de l'Arago. Caune de l'Arago. Tautavel-en-Roussillon, Pyrénées-Orientales, France, Tome IX, Chapitre 14 (14.2). CNRS Éditions, Paris (*in press b*).

Chevalier, T., Lumley, M.-A., 2022c. Le membre inférieur de l'Homme de la Caune de l'Arago. Les fibulas de l'Homme de la Caune de l'Arago (A33, A49, A52-A56, A104, A114, A125, A144, A152). In: Lumley, M.-A. (Ed.), Les restes humains du Pléistocène moyen de la Caune de l'Arago. Caune de l'Arago. Tautavel-en-Roussillon, Pyrénées-Orientales, France, Tome IX, Chapitre 14 (14.3). CNRS Éditions, Paris (*in press c*).
Chevalier, T., Özçelik, K., Lumley, M.-A. de, Kösem, B., Lumley, H. de, Yalçinkaya, I., Taşkiran, H., 2015. The endostructural pattern of a Middle Pleistocene human femoral diaphysis from the Karain E site (Southern Anatolia, Turkey). American Journal of Physical Anthropology 157 (4), 648–658.
Chevalier, T., Tignères, M., 2020. Age-related site-specific modifications in diaphyseal structural properties of the human fibula: furrows and cross-sectional geometry. American Journal of Physical Anthropology 173 (3), 535–555.
Clark, J.D., Beyene, Y., WoldeGabriel, G., Hartk, W.K., Renne, P.R., Gilbert, H., Defleur, A., Suwa, G., Katoh, S., Ludwig, K.R., Boisserie, J.R., Asfawkk, B., White, T.D., 2003. Stratigraphic, chronological and behavioural contexts of Pleistocene *Homo sapiens* from Middle Awash, Ethiopia. Nature 423, 747–752.
Couchoud, I., 2006. Étude pétrographique et isotopique des spéléothèmes du sud-ouest de la France formés en contexte archéologique : contribution à la connaissance des paléoclimats régionaux du stade isotopique 5 (Thèse de doctorat, Sciences de l'Homme et Société). Université Sciences et Technologies, Bordeaux I.
Dougherty, R., Kunzelmann, K., 2007. Computing local thickness of 3D structures with ImageJ. Microscopy and Microanalysis 13, 1678–1679.
Falguères, C., Shao, Q., Hanc, F., Bahain, J.J., Richard, M., Perrenoud, C., Moigne, A.M., Lumley, H. de, 2015. New ESR and U-series dating at Caune de l'Arago, France: a key-site for European Middle Pleistocene. Quaternary Geochronology 30 (Part B), 547–553.
Funk, J.R., Rodney, W.R., Kerrigan, R.J., Crandall, J.R., 2004. The effect of tibial curvature and fibular loading on the tibia index. Traffic Injury Prevention 5 (2), 164–172.
García-Gonzales, R., Rodríguez, L., Carretero, J.M., Arsuaga, J.L., 2016. The ontogeny of femoral strength in Middle Pleistocene humans from Sima de los Huesos (Atapuerca, Spain). In: Proceedings of the European Society for the Study of Human Evolution 5. Alcalá De Henares, Madrid. p. 103.
Garn, S.M., 1970. The Earlier Gain and the Later Loss of Cortical Bone. Charles C. Thomas, Springfield, Ill.
Garn, S.M., Guzman, M.A., Wagner, B., 1969. Subperiosteal gain and endosteal loss in protein-calorie malnutrition. American Journal of Physical Anthropology 30, 153–156.
Goh, J.C.H., Lee, E.H., Ang, E.J., Bayon, P., Pho, R.W., 1992. Biomechanical study of the load-bearing characteristics of the fibula and the effects of fibular resection. Clinical Orthopedics and Related Research 279, 223–228.
Gottschall, J.S., Kram, R., 2005. Ground reaction forces during downhill and uphill running. Journal of Biomechanics 38, 445–452.
Grün, R., Aubert, M., Joannes-Boyau, R., Moncel, M.-H., 2008. High resolution analysis of uranium and thorium concentration as well as U-series isotope distributions in a Neanderthal tooth from Payre (Ardèche, France) using laser ablation ICP-MS. Geochimica et Cosmochimica Acta 72, 5278–5290.
Hammer, Ø., Harper, D., Ryan, P.D., 2001. PAST: Paleontological statistics software package for education and data analysis. Palaeontologica Electronica 4, 1–9.
Hart, N.H., Newton, R.U., Weber, J., Spiteri, T., Rantalainen, T., Dobbin, M., Chivers, P., Nimphius, S., 2020. Functional basis of asymmetrical lower-body skeletal morphology in professional Australian rules footballers. The Journal of Strength and Conditioning Research 34 (3), 791–799.
Hildebrand, T., Rüegsegger, P., 1997. A new method for the model-independent assessment of thickness in three-dimensional images. Journal of Microscopy 185 (1), 67–75.
Holt, B., 2003. Mobility in Upper Paleolithic and Mesolithic Europe: evidence from the lower limb. American Journal of Physical Anthropology 122, 200–215.
Kennedy, G.E., 1985. Bone thickness in *Homo erectus*. Journal of Human Evolution 14, 699–708.
Kontulainen, S., Sievanen, H., Kannus, P., Pasanen, M., Vuori, I., 2002. Effect of long-term impact-loading on mass, size, and estimated strength of humerus and radius of female racquet-sports players: a peripheral quantitative computed tomography study between young and old starters and controls. Journal of Bone Mineral Research 17, 2281–2289.
Lambert, K.L., 1971. The weight-bearing function of the fibula. The Journal of Bone and Joint Surgery 53A (3), 507–513.
Lanyon, L.E., Baggott, D.G., 1976. Mechanical function as an influence on the structure and form of bone. The Journal of Bone and Joint Surgery 58B, 436–443.
Lazenby, R.A., 1990. Continuing periosteal apposition II: the significance of peak bone mass, strain equilibrium, and age-related activity differentials for mechanical compensation in human tubular bones. American Journal of Physical Anthropology 82, 473–484.
Lovejoy, C.O., 1982. Diaphyseal biomechanics of the locomotor skeleton of Tautavel man with comments on the evolution of skeletal changes in Late Pleistocene man. In: L'*Homo erectus* et la place de l'Homme de Tautavel parmi les hominidés fossiles, prétirage, Tome 1. CNRS, Paris447–470.
Lovejoy, C.O., McCollum, M.A., Reno, P.L., Rosenman, B.A., 2003. Developmental biology and human evolution. Annual Review of Anthropology 32, 85–109.
Lovejoy, C.O., Trinkaus, E., 1980. Strength and robusticity of the Neandertal tibia. American Journal of Physical Anthropology 53, 465–470.
Lumley, M.-A. de, 2015. L'homme de Tautavel. Un *Homo erectus* européen évolué. *Homo erectus tautavelensis*. L'anthropologie 119 (3), 303–348.
Lumley, M.-A. de (Ed.), 2022. Les restes humains du Pléistocène moyen de la Caune de l'Arago. Caune de l'Arago. Tautavel-en-Roussillon, Pyrénées-Orientales, France, Tome IX. CNRS Éditions, Paris (in press).
Lumley, M.-A. de, Lamy, P., 1982. Le membre inférieur de l'Homme de Tautavel: fémurs et fibulae. In: L'*Homo erectus* et la place de l'Homme de Tautavel parmi les hominidés fossiles, prétirage, Tome 1. CNRS, Paris276–318.
Lüscher, S.H., Nocciolino, L.M., Pilot, N., Pisani, L., Ireland, A., Rittweger, J., Ferretti, J.L., Cointry, G.R., Capozza, R.F., 2019. Differences in the cortical structure of the whole fibula and tibia between long-distance runners and untrained controls. toward a wider conception of the biomechanical regulation of cortical bone structure. Frontiers in endocrinology 10, 833.
Marchi, D., 2007. Relative strength of the tibia and fibula and locomotor behavior in hominoids. Journal of Human Evolution 53, 647–655.

Please cite this article in press as: Chevalier, T., de Lumley, M.-A., Lower limb bone structure of Middle Pleistocene hominins from the Caune de l'Arago (Tautavel, France): Evolutionary and

Marchi, D., 2015. Variation in tibia and fibula diaphyseal strength and its relationship with arboreal and terrestrial locomotion: extending the investigation to non-hominoid primates. Journal of Anthropological Sciences 93, 153–156.
Marchi, D., Shaw, C.N., 2011. Variation in fibular robusticity reflects variation in mobility patterns. Journal of Human Evolution 61, 609–616.
Marchi, D., Harper, C.M., Chirchir, H., Ruff, C.B., 2019. Relative fibular strength and locomotor behavior in KNM-WT 15000 and OH 35. Journal of Human Evolution 131, 48–60.
Marchi, D., Sparacello, V.S., Shaw, C.N., 2011. Mobility and lower limb robusticity of a pastoralist Neolithic population from North-Western Italy. In: Pinhasi, R., Stock, J.T. (Eds.), Human Bioarchaeology of the Transition to Agriculture. John Wiley and Sons Ltd, Chichester, pp. 317–346.
Martinón-Torres, M., Bermúdez de Castro, J.M., Gómez-Robles, A., Prado-Simón, L., Arsuaga, J.L., 2012. Morphological description and comparison of the dental remains from Atapuerca-Sima de los Huesos site (Spain). Journal of Human Evolution 62, 7–58.
Mednikova, M., Trinkaus, E., 2001. Femoral midshaft diaphyseal cross-sectional geometry of the Sunghir 1 and 4 gravettian human remains. Anthropologie XXXIX/2–3, 103–109.
van der Meulen, M.C.H., Jepsen, K.J., Mikić, B., 2001. Understanding bone strength: Size isn't everything. Bone 29 (2), 101–104.
Nikander, R., Kannus, P., Rantaleinen, T., Uusi-Rasi, K., Heinonen, A., Sievänen, H., 2010. Cross-sectional geometry of weight-bearing tibia in female athletes subjected to different exercise loadings. Osteoporosis International 21, 1687–1694.
Pearson, O.M., Lieberman, D.E., 2004. The aging of Wolff's "Law": ontogeny and responses to mechanical loading in cortical bone. Yearbook of Physical Anthropology 47, 63–99.
Pearson, O.M., Timothy, P.R., Sparacello, V.S., Daneshvari, S.R., Grine, F.E., 2014. Activity, "body shape", and cross-sectional geometry of the femur and tibia. In: Carlson, K.J., Marchi, D. (Eds.), Reconstructing mobility. Springer, New York, pp. 133–151.
Puymerail, L., Condemi, S., Debénath, A., 2013. Analyse comparative structurale des diaphyses fémorales néandertaliennes BD5 (MIS 5e) et CDV-Tour 1 (MIS 3) de La Chaise-de-Vouthon, Charente, France. Paleo 24, 257–270.
Puymerail, L., Ruff, C.B., Bondioli, L., Widianto, H., Trinkaus, E., Macchiarelli, R., 2012a. Structural analysis of the Kresna 11 *Homo erectus* femoral shaft (Sangiran, Java). Journal of Human Evolution 63 (5), 741–749.
Puymerail, L., Volpato, V., Debénath, A., Mazurier, A., Tournepiche, J.-F., Macchiarelli, R., 2012b. A Neanderthal partial femoral diaphysis from the "grotte de la Tour", La Chaise-de-Vouthon (Charente, France): outer morphology and endostructural organization. Comptes Rendus Palévol 11 (8), 581–593.
Rantalainen, T., Weeks, B.J., Nogueira, R.C., Beck, B.R., 2015. Effects of bone-specific physical activity, gender and maturity on tibial cross-sectional bone material distribution: a cross-sectional pQCT comparison of children and young adults aged 5–29 years. Bone 72, 101–108.
Richter, D., Grün, R., Joannes-Boyau, R., Steele, T.E., Amani, F., Rué, M., Fernandes, P., Raynal, J.-P., Geraads, D., Ben-Ncer, A., Hublin, J.-J., McPherron, S.P., 2017. The age of the hominin fossils from Jebel Irhoud, Morocco, and the origins of the Middle Stone Age. Letter 546, 293–296.
Rink, W.J., Schwartz, H.P., Smith, F.H., Radovčić, J., 1995. ESR ages for Krapina hominids. Nature 378, 24.
Rodríguez, L., Carretero, J.M., García-González, R., 2018. Cross-sectional properties of the lower limb bones in the Middle Pleistocene Sima de los Huesos sample (Sierra de Atapuerca, Spain). Journal of Human Evolution 117, 1–12.
Roksandic, M., Radović, P., Lindal, J., Mihailovic, D., 2022. Early Neanderthals in contact: the Chibanian (Middle Pleistocene) hominin dentition from Velika Balanica Cave, Southern Serbia. Journal of Human Evolution 166, 103175.
Rosas, A., Bastir, M., Martinez-Maza, C., Bermúdez de Castro, J.M., 2002. Sexual dimorphism in the Atapuerca-SH hominids: the evidence from the mandibles. Journal of Human Evolution 42, 451–474.
Ruff, C.B., 1981. Structural Changes in the Lower Limb Bones with Aging at Pecos Pueblo (Ph.D. Thesis, University of Pennsylvania). University Microfilms International #8127066, Ann Arbor.
Ruff, C.B., 1992. Biomechanical analyses of archaeological human skeletal samples. In: Saunders, S.R., Katzenburg, A. (Eds.), Skeletal Biology of Past Peoples. Alan R. Liss, New York, pp. 37–58.
Ruff, C., 1995. Biomechanics of the hip and birth in early *Homo*. American Journal of Physical Anthropology 98, 527–574.
Ruff, C.B., 1999. Skeletal structure and behavioral patterns of prehistoric Great Basin populations. In: Hemphill, B.E., Larsen, C.S. (Eds.), Prehistoric Lifeways in the Great Basin Wetlands: Bioarchaeological Reconstruction and Interpretation. University of Utah Press, Salt Lake City, pp. 290–320.
Ruff, C.B., 2000. Body size, body shape, and long bone strength in modern humans. Journal of Human Evolution 38, 269–290.
Ruff, C.B., 2008. Femoral/humeral strength in early African *Homo erectus*. Journal of Human Evolution 54, 383–390.
Ruff, C.B., 2010. Body size and body shape in early hominins-implications of the Gona Pelvis. Journal of Human Evolution 58, 166–178.
Ruff, C.B. (Ed.), 2018a. Skeletal Variation and Adaptation in Europeans Upper Paleolithic to the Twentieth Century. Wiley-Blackwell, Hoboken, NJ.
Ruff, C.B., 2018b. Quantifying skeletal robusticity. In: Ruff, C.B. (Ed.), Skeletal Variation and adapTation in Europeans Upper Paleolithic to the Twentieth Century. Wiley-Blackwell, Hoboken, NJ, (3), pp. 39–47.
Ruff, C.B., Garofalo, E., Niinimäki, S., 2018. Britain. In: Ruff, C.B. (Ed.), Skeletal Variation and Adaptation in Europeans Upper Paleolithic to the Twentieth Century. Wiley-Blackwell, Hoboken, NJ, (8), pp. 209–240.
Ruff, C.B., Hayes, W.C., 1983a. Cross-sectional geometry of Pecos Pueblo femora and tibiae-A biomechanical investigation: I. Method and general patterns of variation. American Journal of Physical Anthropology 60, 359–381.
Ruff, C.B., Hayes, W.C., 1983b. Cross-sectional geometry of Pecos Pueblo femora and tibiae – A biomechanical investigation: II. Sex, age, and side differences. American Journal of Physical Anthropology 60, 383–400.
Ruff, C.B., Holt, B.M., Niskanen, M., Sládek, V., Berner, M., Garofalo, E., Garvin, H.M., Hora, M., Junno, J.-A., Schuplerova, E., Vilkama, R., Whittey, E., 2015b. Gradual decline in mobility with the adoption of food production in Europe. Proceeding of the National Academy of Sciences of the United States of America 112, 7147–7152.
Ruff, C.B., Holt, B.M., Sládek, V., Berne, M., Murphy, W.A., Nedden, D., Seidler, H., Recheis, W., 2006. Body size, body proportions, and mobility in the Tyrolean "Iceman". Journal of Human Evolution 51, 91–101.
Ruff, C.B., Puymerail, L., Macchiarelli, R., Sipla, J., Ciochon, R.L., 2015a. Structure and composition of the Trinil femora: functional and taxonomic implications. Journal of Human Evolution 80, 147–158.

Please cite this article in press as: Chevalier, T., de Lumley, M.-A., Lower limb bone structure of Middle Pleistocene hominins from the Caune de l'Arago (Tautavel, France): Evolutionary and

Ruff, C.B., Trinkaus, E., Walker, A., Larsen, C.S., 1993. Postcranial robusticity in *Homo*. I: temporal trends and mechanical interpretation. American Journal of Physical Anthropology 91, 21–53.
Ruff, C.B., Walker, A., Trinkaus, E., 1994. Postcranial robusticity in *Homo*. III: ontogeny. American Journal of Physical Anthropology 93, 35–54.
Schneider, C.A., Rasband, W.S., Eliceiri, K.W., 2012. NIH Image to ImageJ: 25 years of image analysis. Nature Methods 9, 671–675.
Shackelford, L.L., 2007. Regional variation in the postcranial robusticity of Late Upper Paleolithic humans. American Journal of Physical Anthropology 133, 655–668.
Shaw, C.N., Ryan, T.M., 2012. Does skeletal anatomy reflect adaptation to locomotor patterns? Cortical and trabecular architecture in human and nonhuman anthropoids. American Journal of Physical Anthropology 147, 187–200.
Shaw, C.N., Stock, J.T., 2009a. Intensity, repetitiveness, and directionality of habitual adolescent mobility patterns influence the tibial diaphysis morphology of athletes. American Journal of Physical Anthropology 140, 149–159.
Shaw, C.N., Stock, J.T., 2009b. Habitual throwing and swimming correspond with upper limb diaphyseal strength and shape in modern human athletes. American Journal of Physical Anthropology 140, 160–172.
Shaw, C.N., Stock, J.T., 2011. The influence of body proportions on femoral and tibial midshaft in hunter-gatherers. American of Journal of Physical Anthropology 144, 22–29.
Sparacello, V.S., Marchi, D., 2008. Mobility and subsistence economy: a diachronic comparison between two groups settled in the same geographical area (Liguria, Italy). American Journal of Physical Anthropology 136, 485–495.
Sparacello, V.S., Marchi, D., Shaw, C.N., 2014. The importance of considering fibular robusticity when inferring the mobility patterns of past populations. In: Carlson, K., Marchi, D. (Eds.), Mobility: Interpreting Behavior from Skeletal Adaptations and Environmental Interactions. Springer, New York, pp. 91–110.
Sparacello, V.S., Villotte, S., Shaw, C.N., Fontana, F., Mottes, E., Starnini, E., Dalmeri, G., Marchi, D., 2018. Changing mobility patterns at the Pleistocene-Holocene transition. Lower limb biomechanics of Italian Gravettian and Mesolithic individuals. In: Borgia, V., Cristiani, E. (Eds.), Paleolithic Italy. Advanced Studies on Early Human Adaptation in the Apennine Peninsula. Sidestone Press, Leiden, pp. 357–396.
Stock, J.T., 2006. Hunter-gatherer postcranial robusticity relative to patterns of mobility, climatic adaptation, and selection for tissue economy. American Journal of Physical Anthropology 131, 194–204.
Takebe, K., Nakagawa, A., Minami, H., Kanazawa, H., Hirohata, K., 1984. Role of the fibula in weight-bearing. Clinical Orthopedics and Related Research 184, 289–292.
Thibeault, A., Villotte, S., 2018. Disentangling Cro-Magnon: A multiproxy approach to reassociate lower limb skeletal remains and to determine the biological profiles of the adult individuals. Journal of Archaeological Science: Reports 21, 76–86.
Thomas, K.A., Harris, M.B., Willis, M.C., Lu, Y., MacEwen, G.D., 1995. The effects of the interosseous membrane and partial fibulectomy on loading of the tibia: a biomechanical study. Orthopedics 18 (4), 373–383.
Trinkaus, E., 1997. Appendicular robusticity and the paleobiology of modern human emergence. Proceeding of the National Academy of Sciences of the United States of America 94, 13367–13373.
Trinkaus, E., 2006. Modern human versus Neandertal evolutionary distinctiveness. Current Anthropology 47 (4), 597–620.
Trinkaus, E., Churchill, S.E., Ruff, C.B., 1994. Poscranial robusticity in *Homo*. II: humeral bilateral asymmetry and bone plasticity. American Journal of Physical Anthropology 93, 1–34.
Trinkaus, E., Ruff, C.B., 1989. Diaphyseal cross-sectional morphology and biomechanics of the Fond-de-Forêt 1 femur and the Spy 2 femur and tibia. Anthropologie et Préhistoire 100, 33–42.
Trinkaus, E., Ruff, C.B., 1999. Diaphyseal cross-sectional geometry of near eastern Middle Paleolithic humans: the femur. Journal of Archaeological Science 26, 409–424.
Trinkaus, E., Ruff, C.B., 2012. Femoral and tibial diaphyseal cross-sectional geometry in Pleistocene *Homo*. PaleoAnthropology 13–62.
Trinkaus, E., Sparacello, V.S., Xing, S., Thibeault, A., Villotte, S., 2022. Describing Cro-Magnon: The femora, tibiae and fibulae. Journal of Archaeological Science: Reports 42, 103418.
Valladas, H., Mercier, N., Ayliffe, L., Falgueres, C., Bahain, J.-J., Dolo, J.-M., Froget, L., Joron, J.-L., Masaoudi, H., Reyss, J.-L., Moncel, M.-H., 2008. Radiometric dates for the Middle Paleolithic sequence of Payre (Ardèche, France). Quaternary Geochronology 3, 377–389.
Villotte, S., Samsel, M., Sparacello, V., 2017. The paleobiology of two adult skeletons from Baousso da Torre (Bausu da Ture) (Liguria, Italy): implications for Gravettian lifestyle. Comptes Rendus Palevol 16 (4), 462–473.
Wallace, I.J., Demes, B., Mongie, C., Pearson, O.M., Polk, J.D., Lieberman, D.E., 2014. Exercise-induced bone formation is poorly linked to local strain magnitude in the sheep tibia. PLoS ONE 9 (6), e99108.
Wang, Q., Whittle, M., Cunningham, J., Kenwrigth, J., 1996. Fibula and its ligaments in load transmission and ankle joint stability. Clinical Orthopaedics and Related Research 330, 261–270.
Warden, S.J., Mantila Roosa, S.M., Kersh, M.E., Hurd, A.L., Fleisig, G.S., Pandy, M.G., Fuchs, R.K., 2014. Physical activity when young provides lifelong benefits to cortical bone size and strength in men. Proceeding of the National Academy of Sciences of the United States of America 111 (14), 5337–5442.
Weatherholt, A.M., Warden, S.J., 2016. Tibial bone strength is enhanced in the jump leg of collegiate-level jumping athletes: a within-subject controlled cross-sectional study. Calcified Tissue International 98 (2), 129–139.
Weidenreich, F., 1938. Discovery of the femur and the humerus of *Sinanthropus pekinensis*. Nature 141, 614–617.
Wilks, D.C., Winwood, K., Gilliver, S.F., Kwiet, A., Chatfield, M., Michaelis, I., Sun, L.W., Ferretti, J.L., Sargeant, A.J., Felsenberg, D., Rittweger, J., 2009. Bone mass and geometry of the tibia and the radius of master sprinters, middle- and long-distance runners, race-walkers and sedentary control participants: a pQCT study. Bone 45 (1), 91–97.

Please cite this article in press as: Chevalier, T., de Lumley, M.-A., Lower limb bone structure of Middle Pleistocene hominins from the Caune de l'Arago (Tautavel, France): Evolutionary and